

 Open access • Posted Content • DOI:10.1101/823641

A snapshot of progenitor-derivative speciation in action in *Iberodes* (Boraginaceae)

— [Source link](#) 

Ana Otero, Pablo Vargas, Virginia Valcárcel, Mario Fernández-Mazuecos ...+2 more authors

Institutions: Spanish National Research Council, Autonomous University of Madrid, Morton Arboretum

Published on: 11 Dec 2019 - bioRxiv (Cold Spring Harbor Laboratory)

Topics: Parapatric speciation, Allopatric speciation, Sympatry, Genetic algorithm and Lineage (evolution)

Related papers:

- [Plant budding speciation predominant by ecological and geographical differentiation: an 'evolutionary snapshot' in *Iberodes* \(Boraginaceae\)](#)
- [Speciation-with-Gene-Flow](#)
- [The Geography of Speciation in Neotropical Salamanders](#)
- [Allopatric speciation is more prevalent than parapatric ecological divergence in tropical montane systems \(Asteraceae: Piofontia\)](#)
- [Species and Speciation](#)

Share this paper:    

View more about this paper here: <https://typeset.io/papers/a-snapshot-of-progenitor-derivative-speciation-in-action-in-45fr3p7b8i>

1 **A snapshot of progenitor-derivative speciation in action in *Iberodes* (Boraginaceae)**

2 Ana Otero¹, Pablo Vargas¹, Virginia Valcárcel^{2,3}, Mario Fernández-Mazuecos¹, Pedro
3 Jiménez-Mejías^{2,3} and Andrew L. Hipp^{4,5}

4 ¹ Departamento de Biodiversidad, Real Jardín Botánico, CSIC. Pza. de Murillo, 2,
5 28014 Madrid, Spain

6 ² Centro de Investigación en Biodiversidad y Cambio Global (CIBC-UAM),
7 Universidad Autónoma de Madrid, 28049 Madrid, Spain

8 ³ Departamento de Biología (Botánica), Universidad Autónoma de Madrid, C/Darwin,
9 2, 28049 Madrid, Spain

10 ⁴ The Morton Arboretum, 4100 Illinois Route 53, Lisle, IL 60532, USA

11 ⁵ The Field Museum, 1400 S Lake Shore Drive, Chicago, IL 60605, USA

12

13

14

15 SUMMARY

- 16 • Traditional classification of speciation modes has focused on physical barriers to
17 gene flow. While allopatry has been viewed as the most common mechanism of
18 speciation, parapatry and sympatry, both entail speciation in the face of ongoing
19 gene flow and thus both are far more difficult to detect and demonstrate.
20 *Iberodes* (Boraginaceae, NW Europe) with a small number of recently derived
21 species (five) and contrasting morphological traits, habitats and distribution
22 patterns constitutes an ideal system in which to study drivers of lineage
23 divergence and differentiation.
- 24 • To reconstruct the evolutionary history of the genus, we undertook an
25 integrative study entailing: (i) phylogenomics based on restriction-site
26 associated DNA sequencing (RAD-seq), (ii) morphometrics, and (iii) climatic
27 niche modelling.
- 28 • Key results revealed a history of repeated progenitor-derivative speciation,
29 manifesting in paraphyletic pattern within *Iberodes*. Climatic niche analyses,
30 together with the morphometric data and species distributions, suggest that
31 ecological and geographical differentiation have interacted to shape the diversity
32 of allopatric and parapatric distributions observed in *Iberodes*.
- 33 • Our integrative study has enabled to overcome previous barriers to
34 understanding parapatric speciation by demonstrating the recurrence of
35 progenitor-derivative speciation in plants with gene flow and ecological
36 differentiation, explaining observed parapatry and paraphyly.

37

38 **Keywords:** Budding speciation, ecological speciation, restriction-site associated DNA
39 sequencing (RAD-seq), molecular dating, species distribution modelling, niche overlap,
40 paraphyly, parapatry.

41

42

43

44

45

46

47 INTRODUCTION

48 Understanding what modes of speciation dominate diverse clades across the tree of life
49 has been a contentious domain of evolutionary biology for decades (e.g. Templeton,
50 1981; Rieseberg & Brouillet, 1994; Butlin *et al.*, 2008; Horandl & Stuessy, 2010).
51 Reproductive barriers are the most frequently used criteria for distinguishing among
52 three overarching modes of speciation (Futuyma, 2009). Speciation of adjacent
53 populations in the absence of clear physical or reproductive barriers is frequently
54 explained under the process of (1) parapatric speciation, which entails the evolution of
55 reproductive isolation in the face of limited but ongoing gene flow (Coyne & Orr, 2004,
56 p. 112). Parapatric speciation can be considered intermediate between allopatric and
57 sympatric speciation. In (2) allopatric speciation, gene flow is prevented by geographic
58 barriers between populations. In (3) sympatric speciation, partial or complete
59 reproductive isolation arises between subsets of a single population with overlapping
60 ranges, without spatial segregation. Sympatric speciation often entails significant levels
61 of gene flow at the early stages of differentiation (Gavrilets, 2003; Futuyma, 2009).
62 Whereas allopatry is widely viewed to be the most common mode of speciation (Coyne
63 & Orr, 2004; Vargas *et al.*, 2018), the relative importance of parapatry and sympatry has
64 been the subject of considerable debate (Fitzpatrick *et al.*, 2008; Fitzpatrick *et al.*, 2009;
65 Arnold, 2015) in large part due to the difficulty of (1) resolving phylogenetic
66 relationships among very closely related populations that may still be exchanging genes
67 at a low level, and (2) quantifying the amount of gene flow between populations during
68 population divergence (Barluenga *et al.*, 2006; Fontdevilla, 2014). In the last decade,
69 new genomic, phylogenetic, and ecological tools have made non-allopatric modes of
70 speciation increasingly amenable to study, allowing us to explore with statistical rigor a
71 wider range of speciation scenarios (e.g. Savolainen *et al.*, 2006; Chozas *et al.*, 2017;
72 Zheng *et al.*, 2017). In particular, there are some critical points of evidence that together
73 provide support for a parapatric speciation scenario: (1) phylogenetic relationships
74 usually reflect a progenitor-derivative (budding) pattern in which the more widely
75 distributed species is the living progenitor of the more restricted one; (2) the absence of
76 any physical barrier to gene-flow in both present and past times, i.e. distribution ranges
77 are adjacent; (3) interspecific genetic differentiation that putatively discards processes
78 of secondary contact; (4) alternative forces of reproductive isolation factors—e.g.,
79 differential climatic niches, reproductive exclusion, ploidy variation, among others—are
80 present.

81 Ecological differentiation is often associated with non-allopatric speciation (Sobel
82 *et al.*, 2010; Nosil, 2012; Stankowsky *et al.*, 2015), particularly in plants, because a
83 sessile habit makes plants more sensitive to fine-scale environmental heterogeneity
84 (Anacker & Strauss, 2014). Both the influence of niche conservatism (i.e. retention of
85 ancestral ecological characteristics of species over time, Peterson *et al.*, 1999) and niche
86 evolution (i.e. adaptation of lineages to changes in the environment, Donoghue &
87 Edwards, 2014) have been argued to play a role in speciation and lineage diversification
88 (Wiens & Graham, 2005; Cavender-Bares, 2019). Nevertheless, the contribution of
89 ecological factors as primary drivers of speciation remains more elusive (Mayr, 1954;
90 Pyron & Burbrink, 2010; Yin *et al.*, 2016).

91 The advent of inexpensive phylogenomic approaches in the last decade have made
92 the genetic side of testing recent speciation scenarios tractable (McCormack *et al.*,
93 2013; McVay *et al.*, 2017a). High Throughput Sequencing (HTS) approaches make it
94 possible to analyze loci sampled from the entire genome in reconstructing species trees
95 (Fernández-Mazuecos *et al.*, 2018) and the history of speciation in the face of gene flow
96 (Leroy *et al.*, 2017; Folk *et al.*, 2018; Crowl *et al.*, 2019). Restriction-site associated
97 DNA sequencing (RAD-seq) has contributed particularly strongly to our understanding
98 of recent evolutionary processes, especially in non-model organisms, since a reference
99 genome is not needed for accurate phylogenetic inference (e.g. Fitz-Gibbon *et al.*,
100 2017). RAD-seq has as a consequence been useful in inferring complex speciation
101 histories: repeated cycles of island connectivity and isolation (the pump hypothesis;
102 Papadopoulou & Knowles, 2015), incipient sympatric speciation (Kautt *et al.*, 2016),
103 allopatric speciation despite historical gene flow (Maguilla *et al.*, 2017), ancient
104 introgression among now-extinct species (McVay *et al.*, 2017b).

105 The Mediterranean subendemic genus *Iberodes* M.Serrano, R.Carbajal & S.Ortiz
106 (Boraginaceae, Cynoglossoidae; Serrano *et al.*, 2016) provides an excellent system for
107 studying recent speciation, morphological and ecological differentiation because it is
108 clearly demonstrated to be a recently-derived genus (Chacón *et al.*, 2017; Otero *et al.*,
109 2019a). *Iberodes* comprises five species and one subspecies that differ in geographic
110 ranges (including allopatric and parapatric species) and habitat (ranging from forest
111 understories to scrublands and coastal dunes). Moreover, all species are endangered and
112 narrowly endemic, except for the widely-distributed *I. linifolia* of the Iberian Peninsula
113 and southeastern France (Talavera *et al.*, 2012). Sanger sequencing has failed to resolve
114 phylogenetic relationships among *Iberodes* species because the markers used to date

115 provide minimal variability (Otero *et al.*, 2014; Holstein *et al.*, 2016a; Holstein *et al.*,
116 2016b; Otero *et al.*, 2019a). The question consequently remains as to what is the relative
117 importance of extrinsic geographical and ecological barriers to the complex speciation
118 patterns observed in *Iberodes*. Given the narrow endemism in most *Iberodes* species,
119 we hypothesize that geographic barriers rather than ecological factors have been
120 predominant in the speciation history of *Iberodes*. To test this hypothesis, we aim to: (1)
121 reconstruct phylogenetic relationships of the five species; (2) infer speciation patterns
122 and lineage diversification during the last geological epochs comparing diverse
123 morphologies and ecologies; and (3) evaluate the relative contribution of geographical
124 and ecological processes in speciation.

125

126 **MATERIAL AND METHODS**

127 **Taxon sampling**

128 Based on species distributions, between one and four individuals from one to nine
129 populations were sampled for each of the five species of *Iberodes* including ssp.
130 *gallaecica* and ssp. *littoralis* of *I. littoralis*) (Fig. 1, Table S1, in Supporting
131 Information). Samples of *I. littoralis*, *I. kuzinskyana* and *I. brassicifolia* were collected
132 in the field during 2015 and stored in silica gel until extraction. Since these species are
133 considered threatened according to IUCN criteria (Lopes & Carvalho, 1990; Serrano &
134 Carbajal, 2003; ICNB, 2007; Moreno, 2008; IUCN, 2019; INPN, 2019), permits were
135 obtained prior to collecting. Mature seeds of *I. commutata* were collected in 2015 and
136 germinated in a glasshouse to obtain green leaves for DNA extraction. Both field and
137 herbarium materials were used to represent the large distribution of *I. linifolia* (Table
138 S1). Three species (17 individuals) of the tribe Omphalodeae were included as the
139 outgroup (Otero *et al.*, 2019b): *Omphalodes nitida*, *Myosotidium hortensia*, and
140 *Gyrocaryum oppositifolium* (Table S1).

141 **DNA extraction and RAD library preparation**

142 DNA was extracted from leaf tissue using a modified CTAB protocol from Doyle and
143 Doyle (1987) and Shepherd and Mc Lay (2011), including a precipitation step in
144 isopropanol and ammonium acetate 7.5M at -20°C overnight to improve yield. DNA
145 extractions were visualized and quantified with NanoDrop 2000/2000c (Thermo-Fisher,
146 Waltham, Massachusetts) and Qubit Fluorometric Quantification (Thermo-Fisher,
147 Waltham, Massachusetts) in the *Instituto de Investigaciones Biomédicas* (IIBm, CSIC-
148 UAM). Final DNA sample concentrations were standardized to 10 ng/ul. Preparation of

149 single-end RAD-seq libraries using restriction enzyme *Pst*I from genomic DNA was
150 conducted at Floragenex Inc. (Eugene, Oregon) following Baird *et al.* (2008) and
151 sequenced as single-end, 100-bp reactions on an Illumina HiSeq 2500 at the University
152 of Oregon Genomics & Cells Characterization Core Facility (library C606). Processed
153 data were returned in the Illumina 1.3 variant of the FASTQ format, with Phred quality
154 scores for all bases.

155 **Data clustering**

156 Sequences from Illumina were analyzed in *PyRAD* v. 3.0.6, a *de novo* clustering
157 pipeline with seven main steps that filter and cluster putatively orthologous loci from
158 RAD sequencing reads (Eaton, 2014). This pipeline is able to cluster highly divergent
159 sequences, taking into account indel variation and nucleotide (SNP) variation. It is thus
160 well-suited to the inter- and intraspecific scales addressed in our study. As no evidence
161 of polyploidy was found from flow cytometry, we did not assess sensitivity of paralog
162 detection to sequencing depth or number of heterozygotic positions allowed per loci or
163 shared among individuals. Base calls with a Phred Quality score <20 were replaced by
164 the ambiguous base code (N). Three similarity percentages were set for the clustering
165 (c) threshold of reads: 85%, 90% and 95%. Four levels of minimum coverage (m) of a
166 sample in a final locus (4, 12, 20, 28) were tested for each of the three percentages of
167 clustering similarity, resulting in a fully factorial set of 12 matrices from the
168 combination of filtering parameters, so we could assess sensitivity of our phylogenetic
169 inferences to clustering assumptions. Consensus base calls were made for clusters with
170 a minimum depth of coverage >5. From each parameter combination we obtained three
171 kinds of output: (1) a matrix with all loci retrieved for each individual (concatenated
172 matrix), (2) a matrix with single nucleotide polymorphisms (SNP matrix), and (3) a
173 matrix with one SNP per locus (unlinked SNP matrix). The loci matrix was explored
174 with the RADami (Hipp, 2014) and vegan (Oksanen *et al.*, 2013) packages of R version
175 3.3.2 (R Core Team, 2013).

176 **Phylogenetic analysis**

177 Maximum likelihood analyses of concatenated matrices obtained in *PyRAD* were
178 performed in RAxML v8.2.10 (Stamatakis, 2014) through the Cipres Portal (Miller *et al.*
179 *et al.*, 2010). We used rapid bootstrapping, the GTRGAMMA model, and automatic-stop
180 bootstrapping with the majority rule criterion. We conducted a maximum likelihood
181 analysis for each of the 12 *PyRAD* concatenated matrices. Finally, we compared the
182 topologies based on average bootstrap support (BS). Between the two topologies with

183 average BS>98%, we chose the one maximizing the number of loci (HBS tree) for the
184 remaining phylogenetic-based analyses. Moreover, we used the unlinked SNP matrix
185 from the HBS tree (HBS matrix) to perform a coalescent-based phylogeny using
186 SVDquartets (Chifman & Kubatko, 2014) in PAUP (Swofford, 2001) through the
187 Cipres portal (Miller *et al.*, 2010). For SVDquartets we grouped individuals based on
188 main clades obtained from concatenated analysis in RAxML and evaluated all possible
189 quartets with 100 bootstrap replicates.

190 **Estimates of divergence times**

191 We used penalized likelihood as implemented in TreePL (Smith & O'Meara, 2012) to
192 estimate a time-calibrated tree for all bootstrap trees (with branch lengths) obtained in
193 RAxML from the HBS tree. TreePL is suitable for divergence time estimation when
194 dealing with large amounts of data, such as those yielded by high throughput
195 sequencing RAD-sequencing (Zheng & Wiens, 2015). Two calibration points were
196 used: (1) tribe Omphalodeae (root) (minimum age (minAge) = 9.062; maximum age
197 (maxAge) = 24.4097) and (2) clade *Iberodes* (ingroup) (minAge = 0.6591; maxAge =
198 3.7132) based on the averaged ages and standard deviation inferred in Otero *et al.*
199 (2019a). While secondary calibrations tend to underestimate the uncertainty of the age
200 estimates in the trees from which they are derived, use of multiple secondary
201 calibrations with the full range of uncertainty found in the original study have the
202 potential to recover more accurate clade ages (Schenk, 2016). Average node ages over
203 all posterior trees from the latter study were calculated using *treeStat* from the BEAST
204 v 1.8.2 package (Drummond *et al.*, 2012). We first conducted an analysis under the
205 “prime” option to select the optimal set of parameter values, using random subsample
206 and replicate cross-validation (RSRCV) to identify the best value for the smoothing
207 parameter, lambda. For this first analysis we used the thorough analysis option and set
208 200,000 iterations for penalized likelihood and 5,000 iterations for cross validation. We
209 then repeated the same thorough analysis and iterations but setting the smoothing value
210 of lambda to 10, gradient based (opt) and auto-differentiation based optimizers (optad)
211 to five, and auto-differentiation cross-validation-based optimizers to two (optcvad).
212 Although TreePL does not draw a prior distribution for the phylogenetic tree, we took
213 into account the bootstrapped variance in topology and branch length by running the
214 same TreePL analysis for each bootstrap tree and then a maximum clade credibility tree
215 using the mean heights was reconstructed in *TreeAnnotator* from the BEAST v. 1.8.2
216 package (Drummond *et al.*, 2012). Our dating analysis thus accounts for the uncertainty

217 in branch length that is due to variance in molecular substitution process across the
218 RAD-seq loci used.

219 **Species-level analyses**

220 Phylogenetic inferences showed two cases of paraphyly within the lineage of *I. linifolia*
221 that involved three other taxa (*I. kuzinskyana*, *I. littoralis* ssp. *littoralis* and ssp.
222 *gallaecica*; see results). To evaluate these cases of paraphyly, a set of analyses were
223 done to analyze the degree of genetic, morphological and ecological differentiation
224 among the four taxa involved. Therefore, the following analyses were performed on a
225 subset of data including only these four taxa.

226 **Genetic structure—**

227 The HBS matrix was used to perform a Discriminant Analysis of Principal Components
228 (DAPC) to identify and describe clusters of genetically related individuals (Jombart *et*
229 *al.*, 2010). The format of the HBS matrix was converted from *vcf* to *genlight* with *vcfR*
230 (Knaus & Grünwald, 2017). DAPC analysis was performed in *adegenet* (Jombart,
231 2008). We fixed the number of clusters to four, based on the natural groups of four
232 taxonomic species and subspecies (the Linifolia clade, see results). We used the
233 function ‘optim.a.score’ to estimate the optimal number of principal components for
234 discriminant analysis. We represented genetic differentiation using scatterplots of the
235 principal components and a barplot representing assignment probabilities of individuals
236 to groups (*compoplot*). In addition, analysis of molecular variance (AMOVA) was
237 performed in *Arlequin* v. 3.5.2.1 (Excoffier & Lischer, 2010). AMOVA was run to
238 evaluate the level of genetic differentiation of the paraphyletic *I. linifolia* as a whole
239 with respect to the other two species (*I. kuzinskyana* and *I. littoralis*) of the Linifolia
240 clade. Therefore, we considered only two groups, *I. linifolia* on one hand, and the two
241 coastal species together (*I. kuzinskyana* and *I. littoralis*) on the other. Finally, to
242 evaluate a potential role of historical introgression in determining paraphyly, we
243 conducted D-statistic tests in *PyRAD* (see Methods S1 for details).

244 **Morphometric evaluation—**

245 We performed a morphometric exploration using principal component analysis (PCA).
246 We consulted the taxonomic literature to identify diagnostic characters in *Iberodes*
247 (Talavera *et al.*, 2012). We measured 12 diagnostic macromorphological vegetative and
248 reproductive characters for 111 individuals from 58 vouchers (two different individuals
249 per voucher except for 5 vouchers with only one individual). We averaged measures
250 from each two individuals of the same voucher. As a result, we obtained a final matrix

251 of 58 accessions from 47 locations (74 individuals from 35 locations of *I. linifolia*, 14
252 from five locations of *I. kuzinskyana*, and 23 from seven locations of *I. littoralis*
253 (including the two subspecies) (Fig. 1, Table S2). Ten morphological characters were
254 quantitatively continuous: four vegetative characters (length of stem, leaves and
255 pedicels, and width of leaves) and six reproductive characters (length of fruiting calix,
256 width and length of nutlet, length of nutlet margin, length of the nutlet margin teeth, and
257 hair length). In addition, one binomial character (presence or absence of bracts) and one
258 quantitative, discrete character (hairs per mm² on the abaxial surface of the nutlet) were
259 also considered.

260 PCA was run using the function ‘pcomp’ from Stats R package (R Core Team,
261 2013). Results were visualized with the function ‘ggbiplot’ in the ggbiplot R package
262 (Vu, 2011).

263 ***Climatic niche differentiation and distribution modelling—***

264 Occurrences of the four taxa were collected from GBIF (<https://www.gbif.org/>). We
265 filtered the resulting dataset by removing points suspected to be incorrect, such as those
266 placed clearly outside of the known species distribution range (based on taxonomic
267 literature and databases; Fernández & Talavera, 2012; Muséum National d’Histoire
268 Naturelle, 2003-2019). Additional geographic coordinates were obtained from
269 herbarium material and our own fieldwork data. We also estimated the geographic
270 coordinates of non-georeferenced herbarium specimens, whenever the locality provided
271 could be pinpointed with an accuracy of ± 5 km (Table S3, Fig. 1). To reduce sampling
272 bias, we filtered the dataset by randomly removing points that were within 0.2° latitude
273 or longitude of each other for *I. linifolia* and 0.1° for *I. littoralis* ssp. *littoralis* and ssp.
274 *gallaecica*. Filtering was not applied for *I. kuzinskyana* because of the low number of
275 occurrences. The final dataset after filtering included 115 occurrences of *I. linifolia*, 11
276 of *I. kuzinskyana*, 16 of *I. littoralis* ssp. *littoralis* and 11 of ssp. *gallaecica*.

277 We obtained 19 bioclimatic variables (resolution of 30”) from WorldClim 1.4
278 (<http://www.worldclim.org/>; Hijmans *et al.*, 2006) for the study region (34° to 50° N;
279 11° W to 7° E). To avoid collinearity among bioclimatic variables, we first excluded
280 variables displaying a high correlation coefficient with other variables ($|r| > 0.7$) in the
281 study area (Dormann *et al.*, 2013). Then, we calculated the variance inflation factor
282 (VIF) for each remaining variable using the HH package in R (Heiberger, 2017) and
283 selected variables with VIF <5 following Benítez-Benítez *et al.* (2018). As a result, the
284 following six variables were selected: bio1, bio3, bio4, bio8, bio12 and bio14. We

285 assessed climatic niche overlap among the four taxa by pairwise comparisons. The E-
286 space (i.e. environmental space resulting from the six climatic variables) of each taxon
287 was analyzed in a Principal Component Analysis (PCA) as implemented in the R
288 package *ecospat* (Di Cola *et al.*, 2017). To visualize niche differences along each of the
289 first two principal components, the result was plotted using the *niceOverPlot* function
290 (Fernández-López & Villa-Machío, 2017), which relies on the *ggplot2* package
291 (Wickham, 2016). We calculated values of Schoener's index (D) as a measure of niche
292 overlap (Schoener, 1968; Warren *et al.*, 2008). Then, we conducted tests of niche
293 equivalency and niche similarity using *ecospat* (Di Cola *et al.*, 2017). The niche
294 equivalency test evaluates whether the observed niche overlap is significantly different
295 from a null simulated by randomly reallocating the occurrences of both entities between
296 their ranges (Broennimann *et al.*, 2012; Warren *et al.*, 2008). The niche similarity test
297 checks whether the overlap between two niches is significantly different from the
298 overlap obtained if random shifts within each environmental space are allowed
299 (Schoener, 1968; Warren *et al.*, 2008). In both cases, we tested for niche divergence by
300 using the `alternative="lower"` option. All tests were based on 100 iterations. In
301 similarity tests, both ranges were randomly shifted (`rand.type=1`).

302 In addition, we modeled the potential range of the four taxa of the Linifolia clade
303 under present conditions, which was then projected to last interglacial (LIG, c. 120–140
304 kya) and last glacial maximum (LGM, c. 21 kya) conditions. To this end, we used the
305 same six WorldClim bioclimatic variables employed for niche differentiation analyses,
306 including present layers, LIG layers from Otto-Bliesner *et al.* (2006) and LGM layers
307 based on the CMIP5 project (three global climate models (GCMs): CCSM4, MIROC-
308 ESM and MPI-ESM-P). Resolution was 30" for current and LIG, and 2.5' for LGM
309 layers. We performed species distribution modeling (SDM) using the maximum entropy
310 algorithm, as implemented in Maxent v3.4 (Phillips *et al.*, 2006). We used the same
311 occurrences for each taxon employed for niche differentiation analyses (see above).
312 80% of occurrences for each taxon were used for model training and 20% for model
313 evaluation. For each taxon, ten subsample replicates were run by randomly partitioning
314 the data into a training set and evaluation set, and a mean model was calculated. For the
315 LGM, an average of the three GCMs was calculated. Logistic outputs were converted
316 into presence/absence using the maximum training sensitivity plus specificity logistic
317 threshold.

318 ***Ploidy level estimation—***

319 Flow cytometry was used to estimate genome size, explore the possible role of
320 polyploidization in speciation, and assess the risk of clustering paralogs in RAD-seq *de*
321 *novo* clustering. Earlier cytogenetic studies for three *Iberodes* species showed them to
322 be diploids ($2n=28$ for *I. linifolia*, *I. commutata* and *I. kuzinskyana* (Franco, 1984; Saly,
323 1997; Talavera *et al.*, 2012), and aneuploidy was inferred for *I. littoralis* based on its
324 chromosome count of $2n=24$ (Fernández-Casas, 1975). Nevertheless, some of these
325 references do not cite the plant sources, making it difficult to assess the connection of
326 cytotypes to populations. Individuals of the five *Iberodes* species were cultivated at the
327 glasshouse and five individuals per species were sampled. In addition, samples of the
328 diploid *Solanum lycopersicum* of known genome size ($2n=24$, $2C=1.88-2.07$ pg,
329 Grandillo *et al.*, 2011) were also cultivated to compare standardized results with our
330 study species and estimate genome sizes (Doležel & Bartoš, 2005). We performed a
331 two-step nuclear DNA Content Analysis using Partec Buffer (de Laat *et al.*, 1987) and
332 DAPI fluorochrome through a Cell Lab Quanta SC flow cytometer (Beckman Coulter,
333 Fullerton, CA, USA) equipped with a mercury lamp following the protocol of Doležel
334 *et al.* (2007). Samples were visualized through the Cell Lab Quanta SC Software
335 package. FL1 detector (530 nm / 28 nm; DAPI emission maximum=461) and FL1-Area
336 was used as directly correlated to DNA content. A minimum number of 1000 nuclei for
337 G1 peak were analyzed. Only histograms with a coefficient of variation (CV) lower than
338 10% for the G1 peak were accepted.

339

340 **RESULTS**

341 **Phylogenetic analysis**

342 After filtering and processing all samples under the different parameter combinations in
343 *PyRAD*, 12 matrices of 54 taxa each but varying in numbers of loci and SNPs were
344 analyzed (see Table S4). The same topology was obtained in RAxML from each of the
345 12 matrices, differing only in bootstrap support (BS) values for the nodes (Fig. S1). The
346 highest BS supports and highest number of loci were obtained for the c95m20 matrix
347 (95% similarity within clusters and minimum coverage of 20 samples for a final locus).
348 Consequently, this matrix was used for the remaining phylogenetic analyses (HBS
349 matrix). *Iberodes brassicifolia* was inferred to be the earliest-diverging lineage, sister to
350 a clade that contains *I. commutata* sister to another subclade with the remaining species
351 (Fig. 2). Paraphyly was inferred for *I. linifolia* since a clade including *I. kuzinskyana*

352 and *I. littoralis* is nested within. Likewise, paraphyly was inferred for *I. littoralis* ssp.
353 *gallaecica* since ssp. *littoralis* is nested within populations of subsp. *gallaecica* (Fig. 2).

354 Taxon groups for coalescent-based phylogenetic inference (SVDquartets) were
355 based on the eight main lineages recovered using RAxML (*Iberodes brassicifolia*, *I.*
356 *commutata*, populations of *I. linifolia* from Seville, core clade of *I. linifolia*,
357 populations of *I. linifolia* from southern Spain, populations of *I. linifolia* from central
358 Portugal, *I. kusinskyana*, and *I. littoralis*, Fig. S2). The species tree topology was mostly
359 congruent with the concatenated phylogenetic topology. The only difference was the
360 placement of *I. linifolia* populations from Seville and southern Spain, which were
361 nested within the core of *I. linifolia* (Fig. S2). In any case, paraphyly of *I. linifolia* is
362 still inferred because of the nested position of *I. kusinskyana* and *I. littoralis* sister to
363 populations of *I. linifolia* from Portugal (Fig. S2).

364 **Divergence time estimates**

365 The stem age estimated for *Iberodes* was 17.56 myr (17.26-17.86 Bootstrapped
366 Variance, BV) with a crown age of 5.32 myr (5.32-5.32 BV) (Fig. 2). Crown age
367 estimates for *I. brassicifolia* and *I. commutata* were 1.29 (1.21-1.33 BV) and 2.22 myr
368 (2.17-2.28 BV), respectively. The crown age of the Linifolia clade (*I. linifolia* s.l., *I.*
369 *kusinskyana* and *I. littoralis*) was inferred to be 4.33 myr (4.25-4.59 BV). Divergence
370 time between Portuguese populations of *I. linifolia* and ancestor of the coastal species
371 (*I. kusinskyana* and *I. littoralis*) was estimated at 3.67 myr (3.60-3.85 HPD). The origin
372 of *I. littoralis* ssp. *littoralis*, possibly from an *I. littoralis* ssp. *gallaecica* ancestor, was
373 inferred to have taken place ca. 10,000 years ago (Fig. 2).

374 **Genetic structure**

375 We set four as the *a priori* number of clusters (K=4) based on the four taxa
376 circumscribed within the Linifolia clade. DAPC analysis identified only one optimal
377 principal component for the scatterplot which revealed two well-differentiated clusters:
378 *I. linifolia* (LIN) on the one side, and the coastal *I. kusinskiana* (KUZ) and *I. littoralis*
379 (LIT_LIT, LIT_GAL) on the other (Fig. 3c). Within the coastal species cluster, *I.*
380 *kusinskyana* occupied a position closer to *I. linifolia*, while the two subspecies of *I.*
381 *littoralis* were intermingled (Fig. 3c). Compoplot assigned all individuals of *I. linifolia*
382 to a separate cluster, without admixture (Fig. 3c). The other three clusters were shared
383 among coastal species with different membership probability (Fig. 3c). One of the two
384 individuals of *I. kusinskyana* was uniquely assigned to one of the clusters, whereas the
385 other individual showed a mixed assignment, with admixture of the three genetic groups

386 (Fig. 3c). Most individuals (nine) of both subspecies of *I. littoralis* were placed in the
387 same two clusters, and two of them showed admixture with the same cluster shared by
388 the two samples of *I. kuzinskyana* (Fig. 3c). Given the interdigitated pattern of the two
389 subspecies of *I. littoralis*, we repeated the analysis by considering the two subspecies as
390 part of a single group (K=3) to evaluate the genetic clustering of *I. littoralis* as a genetic
391 group. Compoplot for K=3 assigned most individuals (nine) of *I. littoralis* to the same
392 cluster, while two samples had mixture assignment probability to the cluster of *I.*
393 *kuzinskyana* (Fig. S3). Likewise, AMOVA of the two groups (*I. linifolia* vs coastal
394 species) showed significant among-group variance (58.88%) higher than within-
395 population variance (38.09%) or variance within populations among groups (3.03%),
396 with a fixation index of $F_{ST}= 0.619$ (Table 1). D-statistic tests did not conclusively
397 support a role of historical introgression in determining paraphyletic pattern since
398 ancient introgression was inferred indiscriminately among lineages of *I. linifolia* and
399 both coastland species (see Methods S1).

400 **Morphometric analysis**

401 Principal Component Analysis (PCA) revealed morphological differentiation between
402 the three taxa. *Iberodes linifolia* exhibited the greatest morphological variation, ranging
403 from the two extremes of both PC1 and PC2 compared to the more restricted variation
404 of coastal species that is concentrated in higher scores of PC1 and lower of PC2. Three
405 species of the Linifolia clade were almost completely differentiated, which supports the
406 previous taxonomic observations. *Iberodes linifolia* and *I. littoralis* occupied the two
407 extremes of variation ranging from higher length of vegetative characters, higher nutlet
408 and nutlet teeth sizes for *I. linifolia* to higher length and density of nutlet trichomes and
409 presence of bracts for *I. littoralis* (Fig. 3a). *Iberodes kuzinskyana* occupied an
410 intermediate position between *I. littoralis* and *I. linifolia*, overlapping very slightly with
411 the latter. The two subspecies of *I. littoralis* were intermingled at the highest scores of
412 PC1 and the lowest of PC2 (Fig. 3a).

413 **Climatic niche differentiation and distribution modelling**

414 The two main principal components of the 6 climatic variables explained 73.59%
415 (PC1=48.86% and PC2=24.73%) of the climatic variability in the study region. The
416 variables that contributed most to PC1 were: bio1 (annual mean temperature), bio8
417 (mean temperature of wettest quarter), bio12 (annual precipitation), and bio14
418 (precipitation of the driest month). Bio3 (isothermality) and bio4 (temperature
419 seasonality) were the two variables most related to PC2. The visualization of the E-

420 space showed little overlap among taxa (Fig. 3b). The geographically widespread
421 *Iberodes linifolia* showed the widest niche, whereas the more narrowly distributed
422 coastal species are more restricted in climatic niche space (Fig. 3b). Among coastal
423 species, *I. kuzinskyana* differs from *I. littoralis* in PC1 (less precipitation and higher
424 temperatures for *I. kuzinskyana*) and overlaps with *I. littoralis* ssp. *gallaecica* but not
425 with *I. littoralis* ssp. *littoralis* in PC2 (higher isothermality in *I. kuzinskyana* and *I.*
426 *littoralis* ssp. *gallaecica*). The two subspecies of *I. littoralis* have well-differentiated
427 niches particularly along PC2. *Iberodes kuzinskyana* occupies an intermediate position
428 between *I. linifolia* and *I. littoralis* subsp. *gallaecica*. Thus, *I. kuzinskyana* marginally
429 overlaps *I. linifolia* in those parts of the niche of *I. linifolia* with higher isothermality,
430 lower temperature and higher precipitation. Indeed, minimum niche overlap was
431 inferred between both subspecies of *I. littoralis* and *I. linifolia* due to lower temperature
432 and higher precipitation for coastal taxa. Consequently, although tests of similarity
433 indicated that observed values of niche overlap are not significantly lower than random
434 overlap, all pairwise equivalency tests significantly rejected the equivalency of niches
435 and this is supported by the low values of D obtained (Table 2).

436 The potential ranges for the species of the Linifolia clade in the present are
437 broadly congruent with known geographic distributions, with overlapping distributions
438 of *I. linifolia* and *I. kuzinskyana* (Fig. 4). In contrast, a contraction of distribution ranges
439 was inferred for the LIG, including the disappearance of the potential range of *I.*
440 *littoralis* ssp. *gallaecica* (Fig. 4), but maintaining the overlap and absence of physical
441 barriers between *I. linifolia* and *I. kuzinskyana*. Projections to the LGM showed a range
442 similar to the present one for *I. linifolia* and expanded ranges for both *I. kuzinskyana*
443 and *I. littoralis* ssp. *gallaecica*. The range of *I. littoralis* ssp. *gallaecica* is inferred to
444 have occupied most of the current range of both subspecies in the LGM, before subsp.
445 *littoralis* differentiated from subsp. *gallaecica*.

446 **Ploidy level estimation**

447 Mean peaks of fluorescence, CV values, and genome sizes obtained for each species are
448 summarized in Fig. S4 and Table S5. Fluorescence peaks were similar among all
449 *Iberodes* species, ranging from 45.2 to 62.6 nm for G1. No evidence of duplicated DNA
450 content was observed, suggesting no ploidy differences among taxa or populations.
451 Likewise, similar genome sizes were obtained for the five species ranging from 1.788 to
452 1.980 pg. *Iberodes kuzinskyana* and *I. littoralis* ssp. *littoralis* exhibited the largest and

453 the smallest genome sizes in the genus, respectively. The five species are similar in
454 genome size to the *S. lycopersicum* standard (1.88-2.07 pg, Grandillo *et al.*, 2011).

455

456 **DISCUSSION**

457 Phylogenetic relationships among *Iberodes* species are robustly inferred by RAD-
458 sequencing, which demonstrated the monophyly of populations except for *I. linifolia*.
459 Two early-diverging monophyletic species (*I. brassicifolia* and *I. commutata*) contrast
460 with paraphyly of three species in the Linifolia clade (Fig. 1). The paraphyly of *I.*
461 *linifolia* with respect to *I. kuzinskyana* and *I. littoralis* suggests a progenitor-derivative
462 relationship between the species, with the widespread species giving rise to the coastal
463 endemics in the course of a northward colonization from the coast of Portugal to the
464 west coast of France. Our results provide multiple lines of evidence that support
465 parapatric divergence of the coastland lineage (*I. kuzinskyana*-*I. littoralis* clade): (1)
466 lack of any physical barrier to gene flow between inland and coastland in the present or
467 the past; (2) low level of contemporary gene flow combined with evidence of historical
468 introgression, supporting budding differentiation rather secondary contact; (3) recent
469 niche differentiation from inland habitats with higher temperature seasonality to
470 coastland ones with higher precipitation; (4) paraphyly of *I. linifolia*, which can be
471 interpreted as the extant inland ancestor of the coastland lineage; and (5) incipient
472 morphological differentiation between *I. linifolia* and the coastal lineage. Subsequently,
473 differentiation in allopatry of the two coastal species during the mid-Pleistocene led to
474 the modern-day species *I. kuzinskyana* and *I. littoralis*, most likely mediated by
475 geographic isolation and niche differentiation. Thus ecological and geographic
476 differentiation contributed to both parapatric and allopatric speciation in the clade.

477 **A predominant paraphyletic pattern during *Iberodes* evolution**

478 Our RAD-seq analyses reveal a pattern of predominant paraphyly within the recently
479 diverged Linifolia clade (Fig. 2). While the populations of *I. brassicifolia* and those of *I.*
480 *commutata* form monophyletic groups, paraphyly is inferred for *I. linifolia* populations
481 with respect to the two coastal species. While apparent paraphyly of species may be a
482 consequence of introgression dragging populations toward the species to which they
483 have introgressed (e.g., Eaton *et al.*, 2015), our analyses of historical introgression using
484 *D*-statistics do not conclusively support a role of introgressive hybridization in shaping
485 the paraphyletic topology (Methods S1), and genetic structure shows no evidence of
486 recent admixture involving *I. linifolia* (Fig. 3c). This suggests that *Iberodes* contains

487 some truly paraphyletic species, supporting a progenitor-derivative or “budding”
488 speciation history. Despite the tendency in taxonomy to only consider monophyletic
489 species, paraphyletic ones have been reported as particularly common in groups
490 showing recent local speciation, i.e. groups composed of a ‘mother’ species that
491 coexists in time and space with more restricted derivative species (Rajakaruna, 2018).

492 **Recent ecological speciation in parapatric *Iberodes***

493 Although parapatry has been argued to be common in plants (Rieseberg & Brouillet,
494 1994), few empirical examples are found on the literature (Table 3). Our study provides
495 strong evidence for parapatry through a process of progenitor-derivative (or budding)
496 speciation between *I. linifolia* and the ancestor of *I. kuzinskyana* and *I. littoralis*. Indeed,
497 the projection of distribution models to past climatic periods during the Quaternary
498 revealed a similar or greater degree of geographic overlap between the potential ranges
499 of *I. linifolia* and *I. kuzinskyana* (Fig. 4), which makes allopatry unlikely (Zheng *et al.*,
500 2017). Peripheral populations of the widespread *I. linifolia* close to the coast of Portugal
501 are the most closely related potential living progenitor of the coastal species (*I.*
502 *kuzinskyana* and *I. littoralis*; Fig. 2), which seem to have differentiated in an adjacent
503 area with no apparent physical barrier. Paraphyly similarly supports the hypothesis of
504 budding (progenitor-derivative) speciation (Stuessy & Hörandl, 2013). In addition, the
505 historical introgression inferred among *I. linifolia* and coastland species (Methods S1),
506 does not conclusively underlie the paraphyletic topology. Moreover, our results of
507 AMOVA and DAPC pointed to lack of recent gene flow between the nearby species (*I.*
508 *kuzinskyana* and *I. linifolia*). This pattern supports strong isolation rather than secondary
509 contacts as suggested in other cases of ecological differentiation (e.g. *Mimulus*,
510 Stankowski *et al.*, 2015; *Stauracanthus*, Chozas *et al.*, 2017; Table 3). Nevertheless, a
511 deeper population genetics study focused on the adjacent populations of Portugal is
512 necessary to obtain more detailed estimates of gene flow.

513 In the earliest stages of parapatric speciation mediated by ecological differentiation,
514 reproductive barriers are expected to evolve in response to selection towards locally
515 adapted, divergent ecotypes (Sakaguchi *et al.*, 2019). The niche identity tests point to a
516 role of ecologically-based selection in the speciation of the coastal lineage from *I.*
517 *linifolia*. The coastal lineage is distributed in niches with less temperature seasonality
518 and higher precipitation means than *I. linifolia* (Fig. 3b). Interestingly, although niche
519 overlap is close to zero, similarity tests indicated a certain degree of similarity within
520 the E-space, which points to recent divergence and suggests ongoing differentiation or

521 some degree of niche conservatism. Besides, edaphic factors such as the specialization
522 in coastal dune substrates may also have contributed to ecological differentiation,
523 although this is a fine-scale soil variable that has not been mapped at high enough
524 resolution to include meaningfully in niche models. The differentiation of coastal
525 lineages (*I. kuzinskyana* and *I. littoralis*) from inland populations of *I. linifolia* seems to
526 have started in western Iberian Peninsula during the Mid Pliocene (3.85-3.60 myr, Fig.
527 2), when increasing seasonality led to the origin of Mediterranean climate with its
528 summer droughts (Suc, 1984). The onset of Mediterranean climate favored the
529 differentiation and configuration of modern Mediterranean flora (Vargas *et al.*, 2018),
530 which agrees with recent *Iberodes* speciation (Fig. 2). Posterior glacial/interglacial
531 periods during the Late Pliocene promoted the expansion and contraction of geographic
532 ranges and the formation of sources and sinks of genetic diversity for most
533 Mediterranean species (Médail & Diadema, 2009). Interestingly, the overlapping area
534 inferred for *I. linifolia* and *I. kuzinskyana* in the past is congruent with the location of
535 glacial refugia (Estremadura and Beira litoral) proposed by Médail and Diadema (2009)
536 and plant species previously studied as glacial refugial species (e.g. *Drosophyllum*
537 *lusitanicum*: Müller & Deil, 2001; *Cistus monspeliensis*: Fernández-Mazuecos &
538 Vargas, 2010; Coello *et al.*, unpublished; *Linaria elegans*: Fernández-Mazuecos &
539 Vargas, 2013).

540 In addition, ecological differentiation in parapatric speciation involves divergent
541 natural selection towards contrasting environments that promotes adaptation to different
542 environments and subsequent barriers to gene flow (Schluter, 2001; Rundle & Nosil,
543 2005). The strength of divergent selection can modulate the degree of completeness of a
544 speciation process (Nosil *et al.*, 2009). In our case, both the high interspecific genetic
545 differentiation and clear morphological and ecological divergence (Fig. 3) between
546 inland and coastal species may reflect strong divergent selection promoting rapid
547 speciation (Pliocene-Pleistocene, Fig. 2). Indeed, our study reinforces the common trend
548 for Mediterranean plants in which narrow endemics arise from ecological differentiation
549 of peripheral populations of more widespread progenitor species (Papuga *et al.*, 2018).
550 Moreover, this trend highlights the role of peripheral populations in setting the scene for
551 diversification, thus revealing their conservation value (Debussche & Thompson, 2003).

552

553 **Allopatric differentiation along the Atlantic coast**

554 An allopatric pattern is also found in the Linifolia clade. Given the current separation
555 between ranges of the three coastal taxa (Fig. 1), allopatry seems to have triggered
556 speciation. On the one hand, the widely separated ranges of *I. kuzinskyana* and *I.*
557 *littoralis* subsp. *gallaecica* both in current times and in projections to the LIG (despite
558 probable intermittent contact during the LGM) suggest either a colonization mediated
559 by LDD followed by geographic isolation and niche shift (Fig. 3, 4) or a vicariant
560 process mediated by an early expansion and contraction of distribution ranges. We find
561 similar examples of recent allopatric speciation for both hypotheses: by LDD among
562 coastal Mediterranean flora in the same period (e.g. Jakob *et al.*, 2007; Carnicero *et al.*,
563 2017; Herrando-Moraira *et al.*, 2017); and expansion/contraction of distribution ranges
564 (e.g. Ortiz *et al.*, 2007; Lo Presti & Oberprieler, 2011; Fernández-Mazuecos & Vargas,
565 2011). On the other hand, the allopatric differentiation of the two subspecies of *I.*
566 *littoralis* was likely preceded by an expansion of *I. littoralis* during the LGM, followed
567 by geographic isolation as its range contracted and niche shifted, leading to the
568 differentiation of *I. littoralis* subsp. *littoralis* in more recent times (Fig. 3, 4). In this
569 case, the probable role of long distance dispersal (LDD) is further supported by the fact
570 that the expanded area during the LGM does not seem to have formed a continuous
571 range (Fig. 4). Indeed, unlike inland species of *Iberodes*, the three coastal taxa seem to
572 have specializations for LDD in the form of uncinated hooks (Fig. 1) in the nutlet,
573 related to the attachment to feathers and fur in other closely related Boraginaceae genera
574 (Selvi *et al.*, 2011).

575

576 CONCLUSIONS

577 Our integrative approach provides a comprehensive history of parapatric speciation,
578 which has long posed a challenge to our understanding of ecological speciation. The
579 integration of RAD-sequencing, morphometrics and climatic niche modelling provide
580 strong evidence that progenitor-derivative speciation with gene flow, associated with
581 ecological divergence, shapes the parapatry we observe today in *Iberodes*. Our work
582 thus serves as a model for how integrative studies may serve as a powerful resource for
583 investigating scenarios of non-allopatric processes in other groups of plants. Processes
584 such as budding speciation bring to light the need to extend species concepts to
585 encompass paraphyletic species as natural units of both taxonomic classification and
586 evolutionary history: species in every sense of the word.

587

588 **ACKNOWLEDGEMENTS**

589 We would like to thank those botanists and colleagues that help us with material
590 sampling and particularly, Diana Íñigo, Paola Pérez, Celia Otero, David Vallecillo,
591 Yurena Arjona, Lua López, Joaquín Ramírez, George Hinton, Javier Morente, Manuel
592 Joao Pinto, Ruben Retuerto, Miguel Serrano, Antonio Rivas, Claude Dauge, Asli Koca,
593 Peter Heenan, Enrique Rico, Ester Vega, Santiago Martín-Bravo, Íñigo Pulgar, and Juan
594 Carlos Zamora. Likewise, we would also appreciate the worthy loans provided by
595 numerous herbaria mentioned at supplementary tables. We gratefully acknowledge the
596 work of the lab technicians of Real Jardín Botánico de Madrid, Yolanda Ruiz, Emilio
597 Cano, Jose González, Olga Popova, and Lucía Sastre. We also thank Lucía Checa and
598 Miriam Pérez for the cytometry lab work. We are grateful for the many methodological
599 comments of John McVay, Irene Villa-Machío, Yurena Arjona, Marcial Escudero,
600 Tamara Villaverde, Javier Fernández-López, Alberto Coello, Santiago Martín-Bravo
601 and Carmen Benítez-Benítez. Finally, we would like to thank the researchers of the
602 Herbarium and Center for Tree Science at The Morton Arboretum (Lisle, Illinois,
603 USA), in particular Marlene Hahn for lab assistance, and the Botany Department of the
604 Field Museum (Chicago, Illinois, USA) for accommodating me at the Field Museum
605 and handling the hosting during the lab stay in Chicago. These data were initially
606 analyzed during a research stay by the first author in the Herbarium of The Morton
607 Arboretum and The Field Museum. This study was supported by the Fundación General
608 CSIC and Banco Santander as part of the project titled “Do all endangered species hold
609 the same value?: origin and conservation of living fossils of flowering plants endemic to
610 Spain.”

611 **AUTHOR CONTRIBUTIONS**

612 AO, PJM, VV and PV contributed to developing the question and experimental design.
613 AO led the material collection. AO, MFM and ALH conducted the data analysis. AO
614 wrote the manuscript with the contribution of all authors in both interpretation and
615 writing.

616 **REFERENCES**

617 **Anacker BL, Strauss SY. 2014.** The geography and ecology of plant speciation: range
618 overlap and niche divergence in sister species. *Proceedings of the Royal Society*
619 *B: Biological Sciences* **281**(1778): 20132980.

- 620 **Andrew RL, Rieseberg LH. 2013.** Divergence is focused on few genomic regions
621 early in speciation: incipient speciation of sunflower ecotypes. *Evolution* **67**(9):
622 2468-2482.
- 623 **Arnold ML. 2015.** *Divergence with genetic exchange*. New York, USA: OUP Oxford.
- 624 **Baird NA, Etter PD, Atwood TS, Currey MC, Shiver AL, Lewis ZA, Selker EU,**
625 **Cresko WA, Johnson EA. 2008.** Rapid SNP discovery and genetic mapping
626 using sequenced RAD markers. *PLoS One* **3**: 1-7.
- 627 **Barluenga M, Stölting KN, Salzburger W, Muschick M, Meyer A. 2006.** Sympatric
628 speciation in Nicaraguan crater lake cichlid fish. *Nature* **439**: 719.
- 629 **Benítez-Benítez C, Escudero M, Rodríguez-Sánchez F, Martín-Bravo S,**
630 **Jiménez-Mejías P. 2018.** Pliocene–Pleistocene ecological niche evolution
631 shapes the phylogeography of a Mediterranean plant group. *Molecular Ecology*
632 **27**(7): 1696-1713.
- 633 **Broennimann O, Fitzpatrick MC, Pearman PB, Petitpierre B, Pellissier L, Yoccoz**
634 **NG, Thuiller W, Fortin M-J, Randin C, Zimmermann NE, et al. 2012.**
635 Measuring ecological niche overlap from occurrence and spatial environmental
636 data. *Global Ecology and Biogeography* **21**(4): 481-497.
- 637 **Butlin RK, Galindo J, Grahame JW. 2008.** Review. Sympatric, parapatric or
638 allopatric: the most important way to classify speciation? *Philosophical*
639 *Transactions of the Royal Society B: Biological Sciences* **363**(1506): 2997-3007.
- 640 **Carnicero P, Sáez L, Garcia-Jacas N, Galbany-Casals M. 2017.** Different speciation
641 types meet in a Mediterranean genus: The biogeographic history of *Cymbalaria*
642 (Plantaginaceae). *Taxon* **66**(2): 393-407.
- 643 **Cavender-Bares J. 2019.** Diversification, adaptation, and community assembly of the
644 American oaks (*Quercus*), a model clade for integrating ecology and evolution.
645 *New Phytologist* **221**(2): 669-692.
- 646 **Chacón J, Luebert F, Weigend M. 2017.** Biogeographic Events Are Not Correlated
647 with Diaspore Dispersal Modes in Boraginaceae. *Frontiers in Ecology and*
648 *Evolution* **5**.
- 649 **Chifman J, Kubatko L. 2014.** Quartet inference from SNP data under the coalescent
650 model. *Bioinformatics* **30**(23): 3317-3324.
- 651 **Chozas S, Chefaoui RM, Correia O, Bonal R, Hortal J. 2017.** Environmental niche
652 divergence among three dune shrub sister species with parapatric distributions.
653 *Annals of Botany* **119**(7): 1157-1167.

- 654 **Coyne JA, Orr HA. 2004.** *Speciation*. Sunderland, MA, USA: Sinauer.
- 655 **Crowl AA, Manos PS, McVay JD, Lemmon AR, Lemmon EM, Hipp AL. 2019.**
656 Uncovering the genomic signature of ancient introgression between white oak
657 lineages (*Quercus*). *New Phytologist*.
- 658 **de Laat A, Gohde W, Vogelzack M. 1987.** Determination of ploidy of single plants
659 and plant populations by flow cytometry. *Plant Breeding* **99**(4): 303-307.
- 660 **Debussche M, Thompson JD. 2003.** Habitat differentiation between two closely
661 related Mediterranean plant species, the endemic *Cyclamen balearicum* and the
662 widespread *C. repandum*. *Acta Oecologica* **24**(1): 35-45.
- 663 **Di Cola V, Broennimann O, Petitpierre B, Breiner FT, D'amen M, Randin C,**
664 **Engler R, Pottier J, Pio D, Dubuis A. 2017.** Ecospat: an R package to support
665 spatial analyses and modeling of species niches and distributions. *Ecography*
666 **40**(6): 774-787.
- 667 **Doležal J, Bartoš J. 2005.** Plant DNA flow cytometry and estimation of nuclear
668 genome size. *Annals of Botany* **95**(1): 99-110.
- 669 **Doležal J, Greilhuber J, Suda J. 2007.** Estimation of nuclear DNA content in plants
670 using flow cytometry. *Nature Protocols* **2**(9): 2233.
- 671 **Donoghue MJ, Edwards EJ. 2014.** Biome shifts and niche evolution in plants. *Annual*
672 *Review of Ecology, Evolution, and Systematics* **45**., 547-572.
- 673 **Dormann CF, Elith J, Bacher S, Buchmann C, Carl G, Carré G, Marquéz JRG,**
674 **Gruber B, Lafourcade B, Leitão PJ. 2013.** Collinearity: a review of methods
675 to deal with it and a simulation study evaluating their performance. *Ecography*
676 **36**(1): 27-46.
- 677 **Doyle J, Doyle J. 1987.** A rapid DNA isolation procedure for small quantities of fresh
678 leaf tissue. *Phytochemistry Bulletin* **19**: 11—15.
- 679 **Drummond AJ, Suchard MA, Xie D, Rambaut A. 2012.** Bayesian phylogenetics with
680 BEAUti and the BEAST 1.7. *Molecular Biology and Evolution* **29**: 1969-1973.
- 681 **Eaton DA. 2014.** PyRAD: assembly of de novo RADseq loci for phylogenetic analyses.
682 *Bioinformatics* **30**(13): 1844-1849.
- 683 **Eaton DA, Hipp AL, González-Rodríguez A, Cavender-Bares J. 2015.** Historical
684 introgression among the American live oaks and the comparative nature of tests
685 for introgression. *Evolution* **69**(10): 2587-2601.

- 686 **Excoffier L, Lischer HE. 2010.** Arlequin suite ver 3.5: a new series of programs to
687 perform population genetics analyses under Linux and Windows. *Molecular*
688 *Ecology Resources* **10**(3): 564-567.
- 689 **Excoffier L, Smouse PE, Quattro JM. 1992.** Analysis of molecular variance inferred
690 from metric distances among DNA haplotypes: application to human
691 mitochondrial DNA restriction data. *Genetics* **131**(2): 479-491.
- 692 **Fernández-Casas J. 1975.** Números cromosómicos de plantas españolas. *Anales del*
693 *Instituto Botánico Cavanilles* **32**: 301–307.
- 694 **Fernández-López J, Villa-Machío I 2017.** NiceOverPlot, or when the number of
695 dimensions does matter (R script).
- 696 **Fernández-Mazuecos M, Mellers G, Vigalondo B, Sáez L, Vargas P, Glover BJ.**
697 **2018.** Resolving recent plant radiations: power and robustness of genotyping-by-
698 sequencing. *Systematic Biology* **67**(2): 250-268.
- 699 **Fernández-Mazuecos M, Vargas P. 2011.** Historical isolation versus recent long-
700 distance connections between Europe and Africa in bifid toadflaxes (*Linaria*
701 sect. *Versicolores*). *PLoS One* **6**(7): e22234.
- 702 **Fernández-Mazuecos M, Vargas P. 2010.** Ecological rather than geographical
703 isolation dominates Quaternary formation of Mediterranean *Cistus* species.
704 *Molecular Ecology* **19**(7): 1381-1395.
- 705 **Fernández-Mazuecos M, Vargas P. 2013.** Congruence between distribution modelling
706 and phylogeographical analyses reveals Quaternary survival of a toadflax
707 species (*Linaria elegans*) in oceanic climate areas of a mountain ring range. *New*
708 *Phytologist* **198**(4): 1274-1289.
- 709 **Fernández I, Talavera S. 2012.** *Omphalodes* Mill. In: Talavera S, Andrés C, Arista M,
710 Fernández Piedra M, Gallego M, Ortiz P, Romero Zarco C, Salgueiro F,
711 Silvestre S, Quintanar A eds. *Flora Iberica*. Madrid: Real Jardín Botánico,
712 CSIC, 324-532.
- 713 **Fitz-Gibbon S, Hipp AL, Pham KK, Manos PS, Sork VL. 2017.** Phylogenomic
714 inferences from reference-mapped and de novo assembled short-read sequence
715 data using RADseq sequencing of California white oaks (*Quercus* section
716 *Quercus*). *Genome* **60**(9): 743-755.
- 717 **Fitzpatrick B, Fordyce J, Gavrillets S. 2008.** What, if anything, is sympatric
718 speciation? *Journal of Evolutionary Biology* **21**(6): 1452-1459.

- 719 **Fitzpatrick BM, Fordyce JA, Gavrillets S. 2009.** Pattern, process and geographic
720 modes of speciation. *Journal of Evolutionary Biology* **22**(11): 2342-2347.
- 721 **Folk RA, Soltis PS, Soltis DE, Guralnick R. 2018.** New prospects in the detection and
722 comparative analysis of hybridization in the tree of life. *American Journal of*
723 *Botany* **105**(3): 364-375.
- 724 **Fontdevila A 2014.** Speciation. In: Vargas P, Zardoya R eds. *The tree of life*.
725 Sunderland, MA, USA: Sinauer Associates, 445-456.
- 726 **Franco JA. 1984.** *Nova Flora de Portugal (Continente e Açores). Vol. 2, Clethraceae-*
727 *Compositae*. Lisboa, Portugal: Instituto Superior de Agronomia.
- 728 **Futuyma DJ. 2009.** *Evolution*. Sunderland, MA, USA: Sinauer.
- 729 **Gavrillets S. 2003.** Perspective: models of speciation: what have we learned in 40
730 years? *Evolution* **57**(10): 2197–2215.
- 731 **Grandillo S, Chetelat R, Knapp S, Spooner D, Peralta I, Cammareri M, Pérez O,**
732 **Termolino P, Perez P, Tripodi ML, et al. 2011.** *Solanum* sect. *Lycopersicon*.
733 In: Kole C ed. *Wild Crop Relatives: Genomic and Breeding Resources*. Berlin,
734 Heidelberg: Springer, 129-215.
- 735 **Heiberger RM 2017.** HH: Statistical analysis and data display: Heiberger and Holland.
736 R package v. 3.1-34.
- 737 **Herrando-Moraira S, Carnicero P, Blanco-Moreno JM, Sáez L, Véla E,**
738 **Vilatersana R, Galbany-Casals M. 2017.** Systematics and phylogeography of
739 the Mediterranean *Helichrysum pendulum* complex (Compositae) inferred from
740 nuclear and chloroplast DNA and morphometric analyses. *Taxon* **66**(4): 909-
741 933.
- 742 **Hijmans RJ, Cameron S, Parra J, Jones P, Jarvis A, Richardson K. 2006.** World-
743 Clim version 1.4. *Museum of Vertebrate Zoology of the University of California,*
744 *CIAT, and Rainforest CRC*.
- 745 **Hipp A. 2014.** RADami: R package for phylogenetic analysis of RADseq data. *R*
746 *package version: 1.0-3*.
- 747 **Holstein N, Chacón J, Hilger HH, Weigend M. 2016a.** No longer shipwrecked—
748 *Selkirkia* (Boraginaceae) back on the mainland with generic rearrangements in
749 South American “*Omphalodes*” based on molecular data. *Phytotaxa* **270**: 231-
750 251.

- 751 **Holstein N, Chacón J, Otero A, Jiménez-Mejías P, Weigend M. 2016b.** Towards a
752 monophyletic *Omphalodes*—or an expansion of North American *Mimophytum*.
753 *Phytotaxa* **288**(2): 131-144.
- 754 **Hörandl E, Stuessy TF. 2010.** Paraphyletic groups as natural units of biological
755 classification. *Taxon* **59**(6): 1641–1653.
- 756 **Huang CL, Ho CW, Chiang YC, Shigemoto Y, Hsu TW, Hwang CC, Ge XJ, Chen**
757 **C, Wu TH, Chou CH, Huang HJ, Gojobori T, Osada N, Chiang TY. 2014.**
758 Adaptive divergence with gene flow in incipient speciation of *Miscanthus*
759 *floridulus/sinensis* complex (Poaceae). *The Plant Journal* **80**(5): 834-847.
- 760 **ICNB 2007.** Plano Nacional de Conservação da Flora em Perigo (1º Fase). Relatório
761 Final. Portugal: Instituto da Conservação da Natureza.
- 762 **INPN 2019.** Liste Rouge de la Flore Vasculaire de Poitou-Charentes.
- 763 **IUCN 2019.** IUCN Red List of Threatened Species. Version 2019.1. .
- 764 **Jakob SS, Ihlow A, Blattner FR. 2007.** Combined ecological niche modelling and
765 molecular phylogeography revealed the evolutionary history of *Hordeum*
766 *marinum* (Poaceae)—niche differentiation, loss of genetic diversity, and
767 speciation in Mediterranean Quaternary refugia. *Molecular Ecology* **16**(8):
768 1713–1727.
- 769 **Jombart T. 2008.** Adegenet: a R package for the multivariate analysis of genetic
770 markers. *Bioinformatics* **24**(11): 1403-1405.
- 771 **Jombart T, Devillard S, Balloux F. 2010.** Discriminant analysis of principal
772 components: a new method for the analysis of genetically structured
773 populations. *BMC Genetics* **11**(1): 94.
- 774 **Kautt AF, Machado-Schiaffino G, Torres-Dowdall J, Meyer A. 2016.** Incipient
775 sympatric speciation in Midas cichlid fish from the youngest and one of the
776 smallest crater lakes in Nicaragua due to differential use of the benthic and
777 limnetic habitats? *Ecology and Evolution* **6**(15): 5342-5357.
- 778 **Knaus BJ, Grünwald NJ. 2017.** VCFR: a package to manipulate and visualize variant
779 call format data in R. *Molecular Ecology Resources* **17**(1): 44-53.
- 780 **Leroy T, Roux C, Villate L, Bodénès C, Romiguier J, Paiva JA, Dossat C, Aury**
781 **JM, Plomion C, Kremer A. 2017.** Extensive recent secondary contacts between
782 four European white oak species. *New Phytologist* **214**(2): 865-878.
- 783 **Lo Presti RM, Oberprieler C. 2011.** The central Mediterranean as a phytodiversity
784 hotchpotch: phylogeographical patterns of the *Anthemis secundiramea* group

- 785 (Compositae, Anthemideae) across the Sicilian Channel. *Journal of*
786 *Biogeography* **38**(6): 1109-1124.
- 787 **Lopes MHR, Carvalho MLS, Silva ARP 1990.** Lista de espécies botânicas a proteger
788 em Portugal continental. In SNPRCN. Lisboa, Portugal.
- 789 **Maguilla E, Escudero M, Hipp AL, Luceño M. 2017.** Allopatric speciation despite
790 historical gene flow: Divergence and hybridization in *Carex furva* and *C.*
791 *lucennoiberica* (Cyperaceae) inferred from plastid and nuclear RAD-seq data.
792 *Molecular Ecology* **26**(20): 5646-5662.
- 793 **Mayr E. 1954.** Geographic speciation in tropical Echinoids. *Evolution* **8**(1): 1-18.
- 794 **McCormack JE, Hird SM, Zellmer AJ, Carstens BC, Brumfield RT. 2013.**
795 Applications of next-generation sequencing to phylogeography and
796 phylogenetics. *Molecular Phylogenetics and Evolution* **66**(2): 526-538.
- 797 **McVay JD, Hauser D, Hipp AL, Manos PS. 2017a.** Phylogenomics reveals a complex
798 evolutionary history of lobed-leaf white oaks in western North America.
799 *Genome* **60**(9): 733-742.
- 800 **McVay JD, Hipp AL, Manos PS. 2017b.** A genetic legacy of introgression confounds
801 phylogeny and biogeography in oaks. *Proceedings of the Royal Society B:*
802 *Biological Sciences* **284**(1854): 20170300.
- 803 **Médail F, Diadema K. 2009.** Glacial refugia influence plant diversity patterns in the
804 Mediterranean Basin. *Journal of Biogeography* **36**(7): 1333-1345.
- 805 **Miller MA, Pfeiffer W, Schwartz T. 2010.** Creating the CIPRES Science Gateway for
806 inference of large phylogenetic trees. *Proceedings of the Gateway Computing*
807 *Environments Workshop*: 1-8.
- 808 **Moreno JC coord. 2008.** *Lista Roja 2008 de la flora vascular española*. Madrid, Spain:
809 Dirección General de Medio Natural y Política Forestal (Ministerio de Medio
810 Ambiente, y Medio Rural y Marino, y Sociedad Española de Biología de la
811 Conservación de Plantas).
- 812 **Müller J, Deil U. 2001.** Ecology and structure of *Drosophyllum lusitanicum* (L.) link
813 populations in the southwestern of the Iberian Peninsula. *Acta Botanica*
814 *Malacitana* **26**: 47-68.
- 815 **Muséum National d'Histoire Naturelle 2003-2019.** *Omphalodes littoralis* Lehm.
816 France: Inventaire National du Patrimoine Naturel.
- 817 **Nosil P. 2012.** *Ecological speciation*. New York, USA: Oxford University Press.

- 818 **Nosil P, Harmon LJ, Seehausen O. 2009.** Ecological explanations for (incomplete)
819 speciation. *Trends in ecology and evolution* **24**(3): 145-156.
- 820 **Oksanen J, Blanchet FG, Kindt R, Legendre P, Minchin PR, O'hara R, Simpson**
821 **GL, Solymos P, Stevens MHH, Wagner H. 2013.** Package 'vegan'.
822 *Community ecology package, version 2*(9).
- 823 **Ortiz M, Tremetsberger K, Talavera S, Stuessy T, García-Castaño J. 2007.**
824 Population structure of *Hypochoeris salzmanniana* DC.(Asteraceae), an endemic
825 species to the Atlantic coast on both sides of the Strait of Gibraltar, in relation to
826 Quaternary sea level changes. *Molecular Ecology* **16**(3): 541-552.
- 827 **Otero A, Jiménez-Mejías P, Valcárcel V, Vargas P. 2014.** Molecular phylogenetics
828 and morphology support two new genera (*Memoremea* and *Nihon*) of
829 Boraginaceae s.s. *Phytotaxa* **173**: 241-277.
- 830 **Otero A, Jiménez-Mejías P, Valcárcel V, Vargas P. 2019a.** Being in the right place at
831 the right time? Parallel diversification bursts favored by the persistence of
832 ancient epizoochorous traits and hidden factors in Cynoglossoideae. *American*
833 *Journal of Botany* **106**(3): 438-452.
- 834 **Otero A, Jiménez-Mejías P, Valcárcel V, Vargas P. 2019b.** Worldwide long distance
835 dispersal favored by epizoochorous traits in the biogeographic history of
836 Omphalodeae (Boraginaceae). *Journal of Systematics and Evolution*.
- 837 **Otto-Bliesner BL, Brady EC, Clauzet G, Tomas R, Levis S, Kothavala Z. 2006.**
838 Last glacial maximum and Holocene climate in CCSM3. *Journal of Climate*
839 **19**(11): 2526-2544.
- 840 **Papadopoulou A, Knowles LL. 2015.** Genomic tests of the species-pump hypothesis:
841 recent island connectivity cycles drive population divergence but not speciation
842 in Caribbean crickets across the Virgin Islands. *Evolution* **69**(6): 1501-1517.
- 843 **Papuga G, Gauthier P, Pons V, Farris E, Thompson J. 2018.** Ecological niche
844 differentiation in peripheral populations: a comparative analysis of eleven
845 Mediterranean plant species. *Ecography* **41**(10): 1650-1664.
- 846 **Paule J, Wagner ND, Weising K, Zizka G. 2017.** Ecological range shift in the
847 polyploid members of the South American genus *Fosterella* (Bromeliaceae).
848 *Annals of Botany* **120**(2): 233-243.
- 849 **Peterson AT, J. S, Sánchez-Cordero V. 1999.** Conservatism of Ecological Niches in
850 Evolutionary Time. *Science* **285**: 1265-1267.

- 851 **Phillips SJ, Anderson RP, Schapire RE. 2006.** Maximum entropy modeling of species
852 geographic distributions. *Ecological Modelling* **190**(3-4): 231-259.
- 853 **Pyron AR, Burbrink FT. 2010.** Hard and soft allopatry: physically and ecologically
854 mediated modes of geographic speciation. *Journal of Biogeography* **37**(10):
855 2005-2015.
- 856 **Rajakaruna N. 2018.** Lessons on evolution from the study of edaphic specialization.
857 *The Botanical Review* **84**(1): 39-78.
- 858 **R Core Team 2013.** R: a Language and Environment for Statistical Computing.
- 859 **Richards TJ, Ortiz-Barrientos D. 2016.** Immigrant inviability produces a strong
860 barrier to gene flow between parapatric ecotypes of *Senecio lautus*. *Evolution*
861 **70**(6): 1239-1248.
- 862 **Rieseberg LH, Brouillet L. 1994.** Are many plant species paraphyletic? *Taxon* **43**: 21-
863 32.
- 864 **Rundle HD, Nosil P. 2005.** Ecological speciation. *Ecology Letters* **8**(3): 336-352.
- 865 **Sakaguchi S, Horie K, Ishikawa N, Nishio S, Worth JRP, Fukushima K, Yamasaki
866 M, Ito M, Bonser S. 2019.** Maintenance of soil ecotypes of *Solidago virgaurea*
867 in close parapatry via divergent flowering time and selection against immigrants.
868 *Journal of Ecology* **107**(1): 418-435.
- 869 **Saly F. 1997.** *Étude botanique, cytogénétique et pédologique de l'arc dunaire Gavres-
870 Quiberon. Incidences sur la conservation du patrimoine végétal sauvage.* PhD,
871 Muséum national d'histoire naturelle de Paris France.
- 872 **Savolainen V, Anstett M-C, Lexer C, Hutton I, Clarkson JJ, Norup MV, Powell
873 MP, Springate D, Salamin N, Baker WJ. 2006.** Sympatric speciation in palms
874 on an oceanic island. *Nature* **441**(7090): 210.
- 875 **Schenk JJ. 2016.** Consequences of secondary calibrations on divergence time
876 estimates. *PLoS One* **11**(1): e0148228.
- 877 **Schulte LJ, Clark JL, Novak SJ, Jeffries SK, Smith JF. 2015.** Speciation within
878 *Columnea* section *angustiflora* (Gesneriaceae): islands, pollinators and climate.
879 *Molecular Phylogenetics and Evolution* **84**: 125-144.
- 880 **Schluter D. 2001.** Ecology and the origin of species. *Trends in Ecology and Evolution*
881 **16**(7): 372-380.
- 882 **Schoener TW. 1968.** The *Anolis* lizards of Bimini: resource partitioning in a complex
883 fauna. *Ecology* **49**(4): 704-726.

- 884 **Selvi F, Coppi A, Cecchi L. 2011.** High epizoochorous specialization and low DNA
885 sequence divergence in mediterranean *Cynoglossum* (Boraginaceae): Evidence
886 from fruit traits and ITS region. *Taxon* **60**: 969-985.
- 887 **Serrano M, Carbajal R 2003.** *Omphalodes littoralis* subsp. *gallaecica* M. Laínz. In:
888 Bañares Á, Blanca G, Güemes J, Moreno JC, Ortiz S eds. *Atlas y Libro Rojo de*
889 *la Flora Vasculare Amenazada de España*. Madrid, Spain: Dirección General de
890 Conservación de la Naturaleza., 274-275.
- 891 **Serrano M, Carbajal R, Pereira-Coutinho A, Ortiz S. 2016.** Two new genera in the
892 *Omphalodes* group (Cynoglosseae, Boraginaceae). *Nova Acta Científica*
893 *Compostelana (Biología)* **23**: 1-14.
- 894 **Shepherd LD, Mc Lay TG. 2011.** Two micro-scale protocols for the isolation of DNA
895 from polysaccharide-rich plant tissue. *Journal of Plant Research* **124**(2): 311-
896 314.
- 897 **Smith SA, O’Meara BC. 2012.** treePL: divergence time estimation using penalized
898 likelihood for large phylogenies. *Bioinformatics* **28**(20): 2689-2690.
- 899 **Sobel JM, Chen GF, Watt LR, Schemske DW. 2010.** The biology of speciation.
900 *Evolution* **64**(2): 295-315.
- 901 **Sobel JM, Streisfeld MA. 2015.** Strong premating reproductive isolation drives
902 incipient speciation in *Mimulus aurantiacus*. *Evolution* **69**(2): 447-461.
- 903 **Stamatakis A. 2014.** RAxML version 8: a tool for phylogenetic analysis and post-
904 analysis of large phylogenies. *Bioinformatics* **30**(9): 1312-1313.
- 905 **Stankowski S, Sobel JM, Streisfeld MA. 2015.** The geography of divergence with
906 gene flow facilitates multitrait adaptation and the evolution of pollinator
907 isolation in *Mimulus aurantiacus*. *Evolution* **69**(12): 3054-3068.
- 908 **Stuessy TF, Hörandl E. 2013.** The importance of comprehensive phylogenetic
909 (evolutionary) classification—a response to Schmidt-Lebuhn’s commentary on
910 paraphyletic taxa. *Cladistics*: 1-3.
- 911 **Suc JP. 1984.** Origin and evolution of the Mediterranean vegetation and climate in
912 Europe. *Nature* **307**(5950): 429.
- 913 **Swofford DL. 2001.** Paup*: Phylogenetic analysis using parsimony (and other
914 methods) 4.0. B5.
- 915 **Talavera S, Andrés C, Arista M, Fernández Piedra M, Gallego M, Ortiz P,**
916 **Romero Zarco C, Salgueiro F, Silvestre S, Quintanar A 2012.** Boraginaceae.
917 In: Talavera S, Andrés C, Arista M, Fernández Piedra M, Gallego M, Ortiz P,

- 918 Romero Zarco C, Salgueiro F, Silvestre S, Quintanar A eds. *Flora Iberica*.
919 Madrid: Real Jardín Botánico, CSIC, 324-532.
- 920 **Templeton AR. 1981.** Mechanisms of speciation- a population genetic approach.
921 *Annual Review of Ecology and Systematics* **12**: 23-48.
- 922 **Vargas P, Fernández-Mazuecos M, Heleno R. 2018.** Phylogenetic evidence for a
923 Miocene origin of Mediterranean lineages: species diversity, reproductive traits
924 and geographical isolation. *Plant Biology* **20**: 157-165.
- 925 **Vu VQ. 2011.** ggbiplot: A ggplot2 based biplot. *R package*.
- 926 **Warren DL, Glor RE, Turelli M. 2008.** Environmental niche equivalency versus
927 conservatism: quantitative approaches to niche evolution. *Evolution* **62**(11):
928 2868-2883.
- 929 **Wickham H. 2016.** *ggplot2: elegant graphics for data analysis*. Switzerland: Springer.
- 930 **Wiens JJ, Graham CH. 2005.** Niche Conservatism: Integrating Evolution, Ecology,
931 and Conservation Biology. *Annual Review of Ecology, Evolution, and*
932 *Systematics* **36**(1): 519-539.
- 933 **Yin H, Yan X, Zhang W, Shi Y, Qian C, Yin C, Tian F, Wang X, Ma X-F. 2016.**
934 Geographical or ecological divergence between the parapatric species *Ephedra*
935 *sinica* and *E. intermedia*? *Plant Systematics and Evolution* **302**(8): 1157-1170.
- 936 **Zheng H, Fan L, Milne RI, Zhang L, Wang Y, Mao K. 2017.** Species Delimitation
937 and Lineage Separation History of a Species Complex of Aspens in China.
938 *Frontiers in Plant Sciences* **8**: 375.
- 939 **Zheng XM, Ge S. 2010.** Ecological divergence in the presence of gene flow in two
940 closely related *Oryza* species (*Oryza rufipogon* and *O. nivara*). *Molecular*
941 *Ecology* **19**(12): 2439-2454.
- 942 **Zheng Y, Wiens JJ. 2015.** Do missing data influence the accuracy of divergence-time
943 estimation with BEAST? *Molecular Phylogenetics and Evolution* **85**: 41-49.
- 944
945
946
947
948
949
950

951 **FIGURE LEGENDS**

952 **Fig. 1** Locations of the *Iberodes* species sampled for the different analyses performed.
953 The star symbols indicate locations for RAD-sequencing, squares represent the
954 locations for the morphometric analysis, and circles indicate locations for the ecological
955 niche modelling. Color legend for each taxa of *Iberodes* is shown in the figure. Images
956 of the six taxa are framed following each taxa color in the map.

957 **Fig. 2** Time-calibrated phylogeny obtained from TreePL by using maximum clade
958 credibility from 1000 bootstrap trees of the maximum likelihood analysis of c95m20
959 matrix. Branch thickness indicates the ML bootstrap supports above 98. Node bars in
960 blue indicate the node age ranges taking into account the branch length variance along
961 the 1000 bootstrap trees. No branch length variation was inferred for nodes without blue
962 bar. The international stratigraphic scale is included from 26 myr until present. Text
963 codes for each individual location are detailed in the Table S1. The color for each
964 lineage of the Linifolia clade is geographically represented through the colored ellipses
965 of the map. Grey ellipses group the different lineages of the four taxa within the
966 Linifolia clade.

967 **Fig. 3** Morphometric, niche overlap and genetic clustering analyses of the Linifolia
968 clade. Codes for each taxa are: LIN for *I. linifolia*, KUZ for *I. kuzinskyana*, LIT-GAL
969 for *I. littoralis* ssp. *gallaecica*, and LIT-LIT for *I. littoralis* ssp. *littoralis*. (a)
970 Morphometric analysis. Principal Component Analysis (PCA) of the 12 morphologic
971 characters: LS, length of the stem; LL, length of the leaf; WL, wide of the leaf; PINFL,
972 pedicel of inflorescence; LCFR, length of fruit calix; DN, diameter of the nutlet; LN,
973 length of the nutlet; LM, length of the margin nutlet; LT, length of the margin teeth;
974 DH, density of trichomes; LH, length of trichome; BR: absence=0, presence=1 of
975 flowering bracts). The contribution of each trait to the two principal components (PC1,
976 PC2) as well as the positive or negative sense of the relationship is represented through
977 the length of each arrow and the directionality of the arrow, respectively. The
978 percentages of the variability explained by the two PCs are indicated close to the axes.
979 (b) Niche overlap analysis. PCA of the six climatic variables obtained from WorldClim.
980 BIO1, Annual Mean Temperature; BIO3, Isothermality; BIO4, Temperature
981 Seasonality; BIO8, Mean Temperature of Wettest Quarter; BIO12, Annual
982 Precipitation; BIO14, Precipitation of Driest Month. The strength of contribution of
983 each variable to PCs and the sense of the relationship is represented, as explained above,
984 through the length and the directionality of the arrows. The percentages of the

985 variability explained by the two PCs are indicated close to the axes. Values of the
 986 variables are also represented for each PC separately following Fernández-López and
 987 Villa-Machío (2017). (c) Genetic clustering. Scatterplot from the DAPC analysis
 988 showing the genetic differentiation retained in one PC as the optimal number of PC for
 989 the discriminant function. Compoplot for K=4 is also represented indicating
 990 membership probability to each genetic cluster for each taxa.

991 **Fig. 4** Species distribution modelling obtained through the entropy algorithm, as
 992 implemented in Maxent for the four taxa of the Linifolia clade. Codes for each taxa are:
 993 LIN for *I. linifolia*, KUZ for *I. kuzinskyana*, and LIT for *I. littoralis* (LIT-GAL for *I.*
 994 *littoralis* ssp. *gallaecica*, LIT-LIT for *I. littoralis* ssp. *littoralis*). Analyses are based on
 995 WorldClim and projected to past conditions: last interglacial (LIG, c. 120–140 kya) and
 996 last glacial maximum (LGM, c. 21 kya). The presence/absence was estimated using the
 997 maximum training sensitivity plus specificity logistic threshold. The projection to the
 998 past is only presented according to the inferred times of divergence of each taxa.

999

1000 TABLES

1001 **Table 1** Analysis of molecular variance (AMOVA) results for individuals from two
 1002 contrasted groups: (1) mainland, *I. linifolia* and (2) coastal, *I. kuzinskyana* and *I.*
 1003 *littoralis*.

1004

Source of Variation	d.f.	Sum of squares	Variance components	Percentage of variation
Among groups	1	1602.666	106.33509 Va	58.88
Among populations within groups	2	181.372	5.47321 Vb	3.03
Within populations	24	1651.033	68.79306 Vc	38.09
Total	27	3435.071	180.60135	

1005 Note: Variance components are as in Excoffier *et al.* (1992). Fst = 0.61909; Fsc = 0.07370; Fct
 1006 = 0.58878.

1007

1008

1009

1010 **Table 2** Pairwise statistical test for comparison of ecological niche overlap between the
 1011 different taxa within the Linifolia clade. The statistical significance is represented by p-
 1012 values (Warren *et al.*, 2008). Asterisk (*) indicate significant values for p -values < 0.01.

Taxa comparison	Schoener's D	Niche equivalency p-value	Niche similarity p-value
<i>I. linifolia</i> vs <i>I. kuzinskyana</i>	0.026	0.0099*	0.94059
<i>I. linifolia</i> vs <i>I. littoralis</i> ssp. <i>gallaecica</i>	0.003	0.003	0.60396
<i>I. linifolia</i> vs <i>I. littoralis</i> ssp. <i>littoralis</i>	0.004	0.0099*	0.69307
<i>I. kuzinskyana</i> vs <i>I. littoralis</i> ssp. <i>gallaecica</i>	0.000	0.0099*	0.64356
<i>I. kuzinskyana</i> vs <i>I. littoralis</i> ssp. <i>littoralis</i>	0.000	0.0099*	0.71287
<i>I. littoralis</i> ssp. <i>gallaecica</i> vs <i>I. littoralis</i> ssp. <i>littoralis</i>	0.000	0.0099*	0.67327

1013

1014 **Table 3** Examples of parapatric speciation in plants.

Genus	Family	Event suggested	Reference
<i>Ephedra</i>	Ephedraceae	Ecological divergence mediated by bioclimatic niche	Yin <i>et al.</i> (2016)
<i>Fosterella</i>	Bromeliaceae	Ecological divergence mediated by polyploidization and	Paule <i>et al.</i> (2017)
<i>Helianthus</i>	Asteraceae	Ecological divergence mediate by bioclimatic niche	Andrew & Rieseberg (2013)
<i>Mimulus</i>	Phrymaceae	Ecological divergence mediated by pollinator shift	Sobel & Streisfeld (2015), Stankowski <i>et al.</i> (2015)
<i>Miscanthus</i>	Poaceae	Ecological divergence mediated by bioclimatic	Huang <i>et al.</i> (2014)

niche			
<i>Oryza</i>	Poaceae	Ecological divergence mediated by bioclimatic niche	Zheng & Ge (2010)
<i>Populus</i>	Salicaceae	Ecological divergence mediated by bioclimatic niche	Zheng <i>et al.</i> (2017)
<i>Roscoea</i>	Zingiberaceae	Ecological divergence mediated by bioclimatic niche	Zhao <i>et al.</i> (2016)
<i>Senecio</i>	Asteraceae	Ecological divergence mediated by ecological niche	Richards & Ortiz-Barrientos (2016)
<i>Stauracanthus</i>	Fabaceae	Ecological divergence mediated by bioclimatic niche	Chozas <i>et al.</i> (2017)
<i>Columnnea</i>	Gesneriaceae	Ecological divergence mediated by bioclimatic niche and pollinator shift	Schulte <i>et al.</i> (2015)

1015

1016

1017 SUPPORTING INFORMATION

1018 Additional Supporting Information may be found online in the Supporting Information
1019 section at the end of the article.

1020 **Fig. S1** RAxML trees of *Iberodes* using three different similarity percentages (85%,
1021 90%, 95%) and four levels of minimum coverage (m4, m12, m20, m28). Bootstrap
1022 support are indicated when is lower than 100.

1023 **Fig. S2.** SVDquartets species tree of *Iberodes* using the eight main lineages obtained in
1024 the RAxML analyses.

1025 **Fig. S3** Compplot showing individual assignment probability to different species-
1026 groups of the Linifolia clade of *Iberodes*, considering the two subspecies of *I. littoralis*
1027 as one group (k=3). Codes for each taxa are: LIN for *I. linifolia*, KUZ for *I.*
1028 *kuzinskyana*, LIT-GAL for *I. littoralis* ssp. *gallaecica*, and LIT-LIT for *I. littoralis* ssp.
1029 *littoralis*.

1030 **Fig. S4** Flow cytometry peaks for each of five samples used for each of the five species
1031 of *Iberodes* (including the two subspecies of *I. littoralis*. Peak of the standard *Solanum*
1032 *lycopersicum* is included. FL1 in the X axis indicates the signal intensity (530 nm / 28
1033 nm; DAPI emission maximum=461). Y axis indicates the number of events found.
1034 Mean, mode, and median values of FL and percentage of variation coefficient is shown
1035 for each colored peak.

1036 **Table S1** Data information and NCBI SRA accession numbers of all individuals
1037 sampled for RADseq.

1038 **Table S2** Morphological characters analyzed. Values represent the mean of two
1039 individuals measured per herbarium sheet. LS: length of the stem, LL: length of the leaf,
1040 WL: wide of the leaf, PINFL: pedicel of inflorescence, LCFR: length of fruit calix, DN:
1041 diameter of the nutlet, LN: length of the nutlet, LM: length of the margin nutlet, LT:
1042 length of the margin teeth, DH: density of the hair, LH: length of trichome.

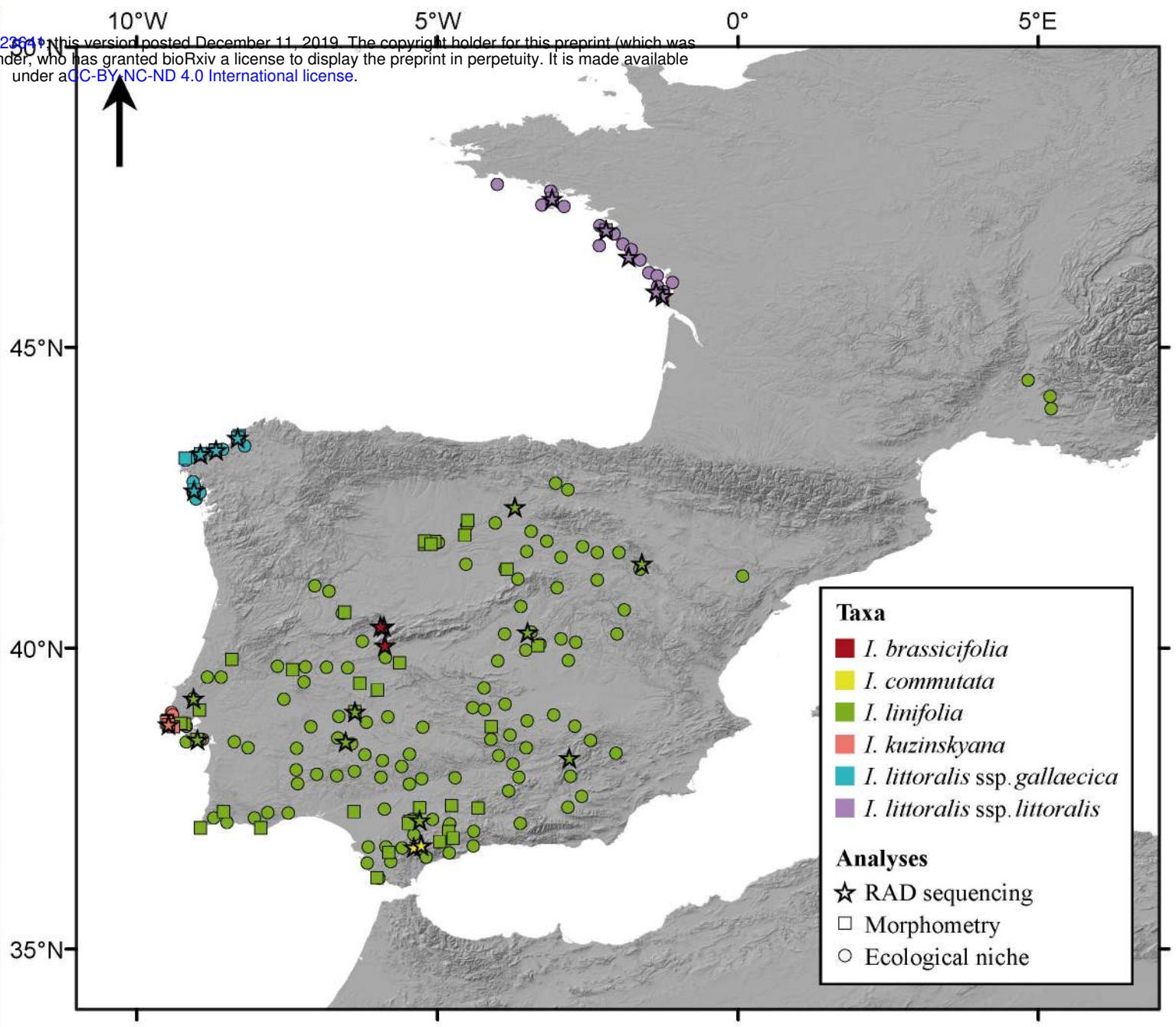
1043 **Table S3** Data points for environmental analysis

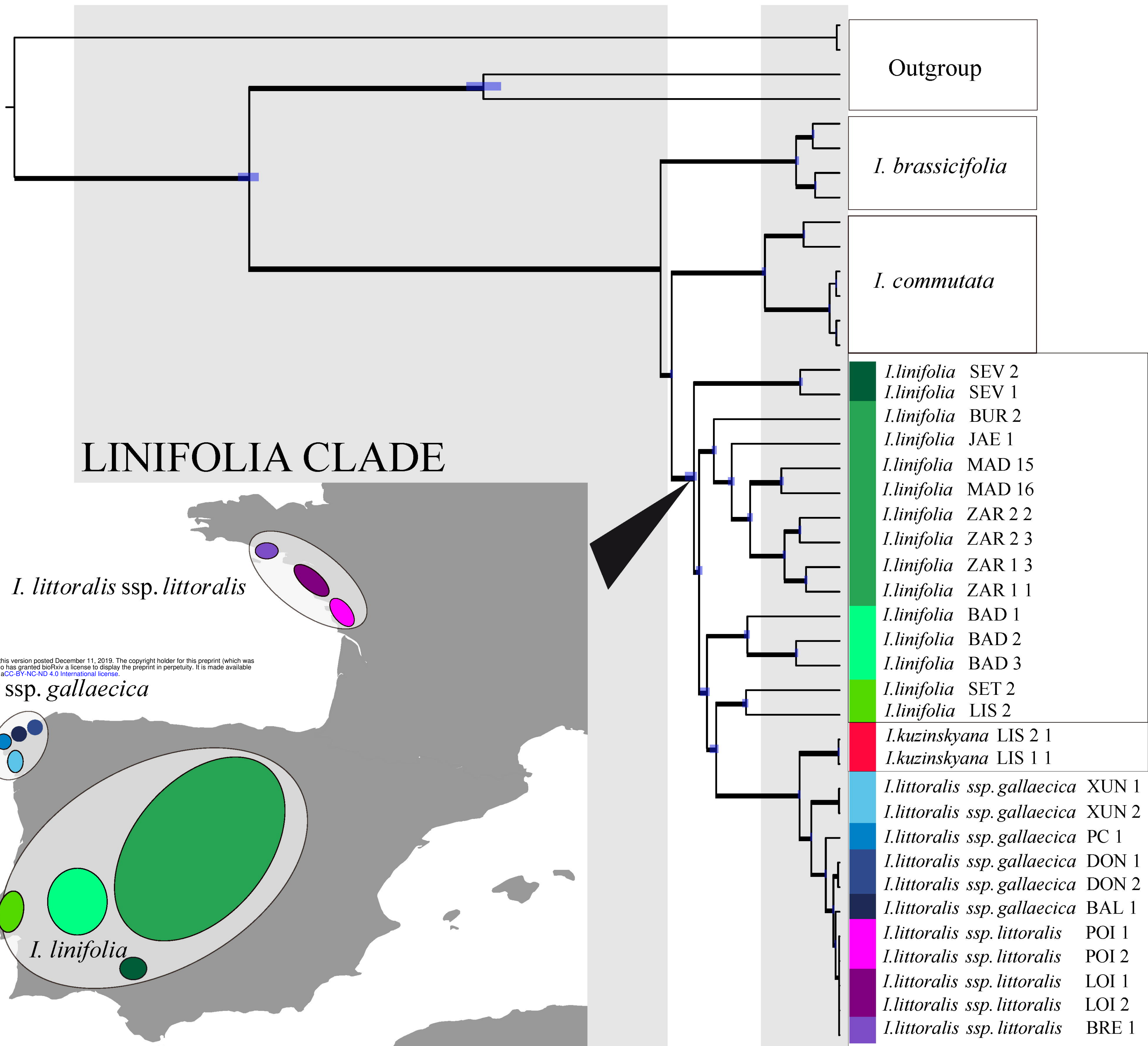
1044 **Table S4** Number of loci, SNPs retrieved for each of the 12 parameter combinations.
1045 Parameter abbreviations indicate: c, clustering threshold; m, minimum taxon coverage to
1046 consider a locus.

1047 **Table S5** Genome size estimation for the five species of *Iberodes* (including the two
1048 subspecies of *I. littoralis*.

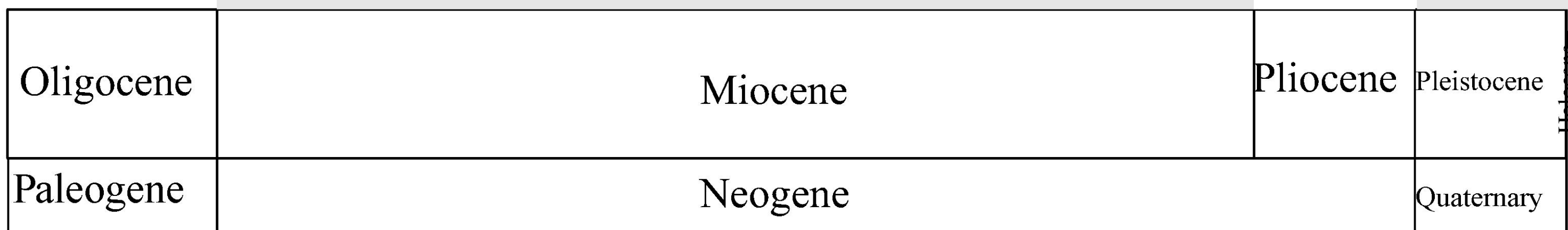
1049 **Methods S1** Introgression analysis.

bioRxiv preprint doi: <https://doi.org/10.1101/82364>; this version posted December 11, 2019. The copyright holder for this preprint (which was not certified by peer review) is the author/funder, who has granted bioRxiv a license to display the preprint in perpetuity. It is made available under aCC-BY-NC-ND 4.0 International license.





bioRxiv preprint doi: <https://doi.org/10.1101/823641>; this version posted December 11, 2019. The copyright holder for this preprint (which was not certified by peer review) is the author/funder, who has granted bioRxiv a license to display the preprint in perpetuity. It is made available under aCC-BY-NC-ND 4.0 International license.



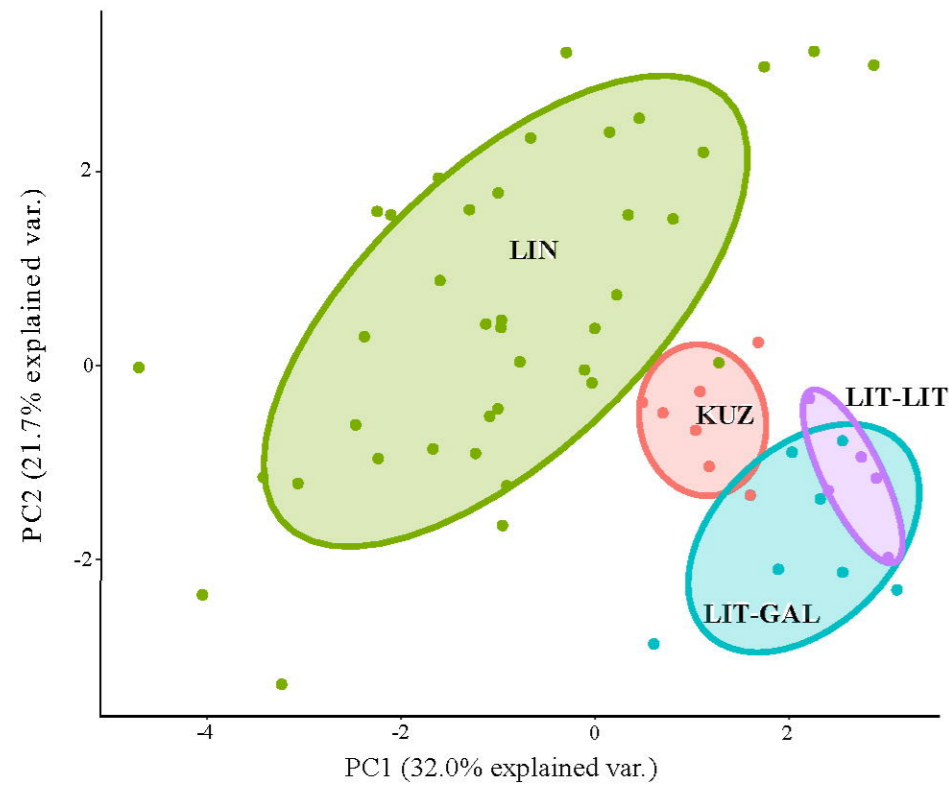
20

10

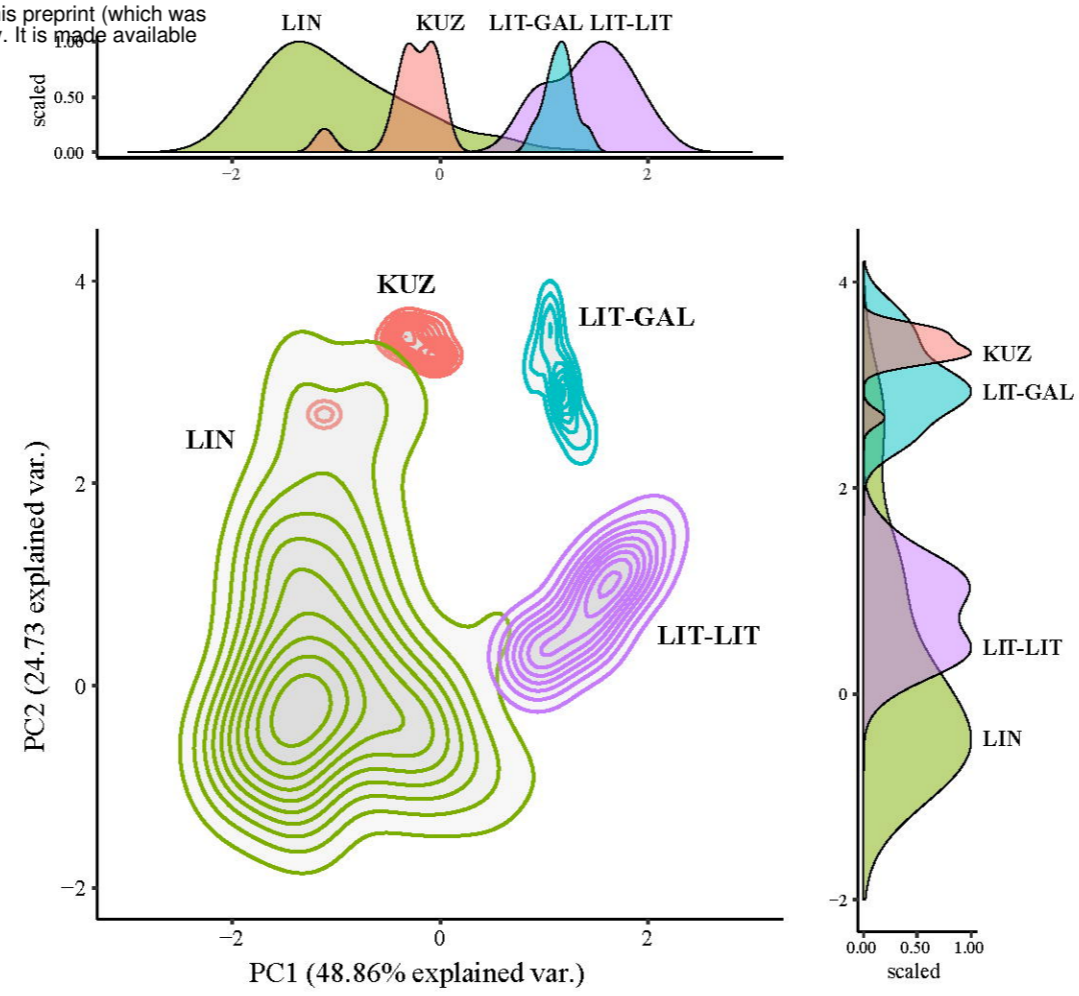
0 (myr)

(a) Morphometric analysis

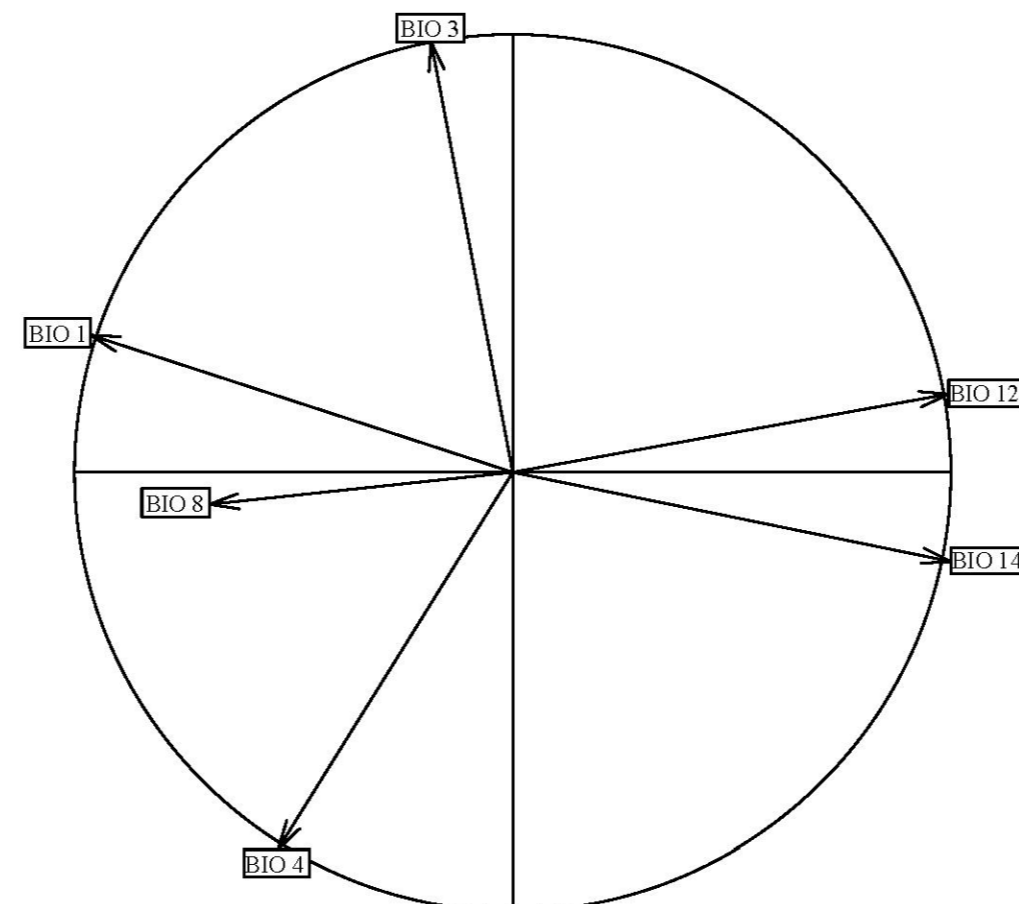
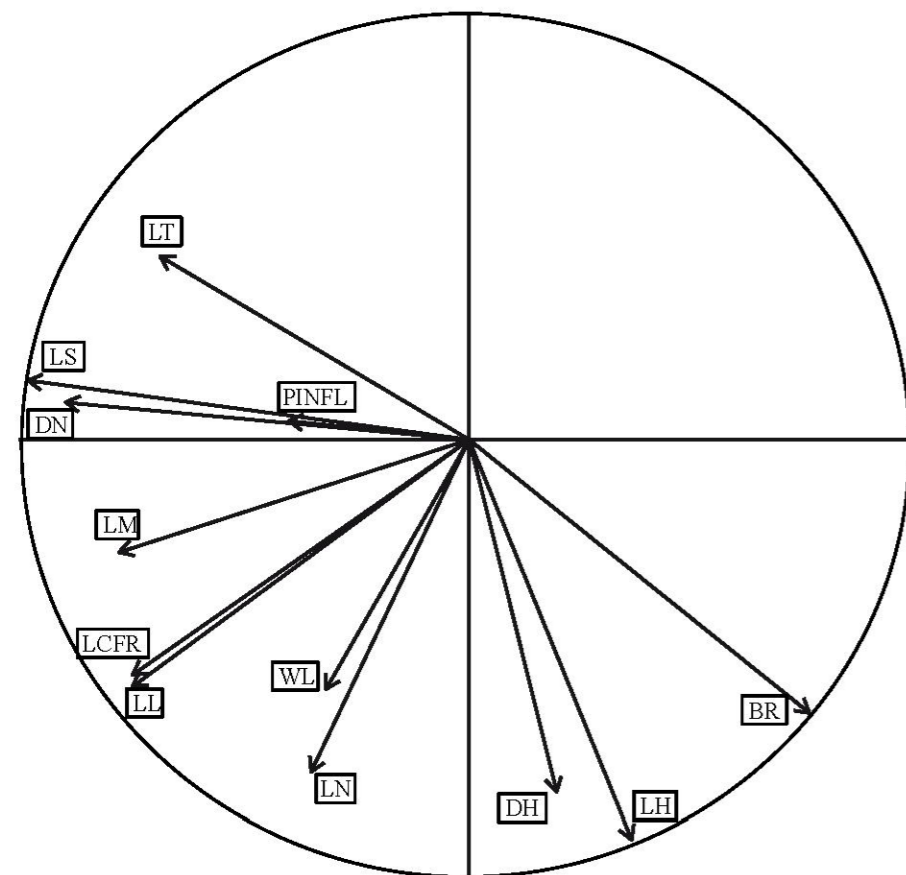
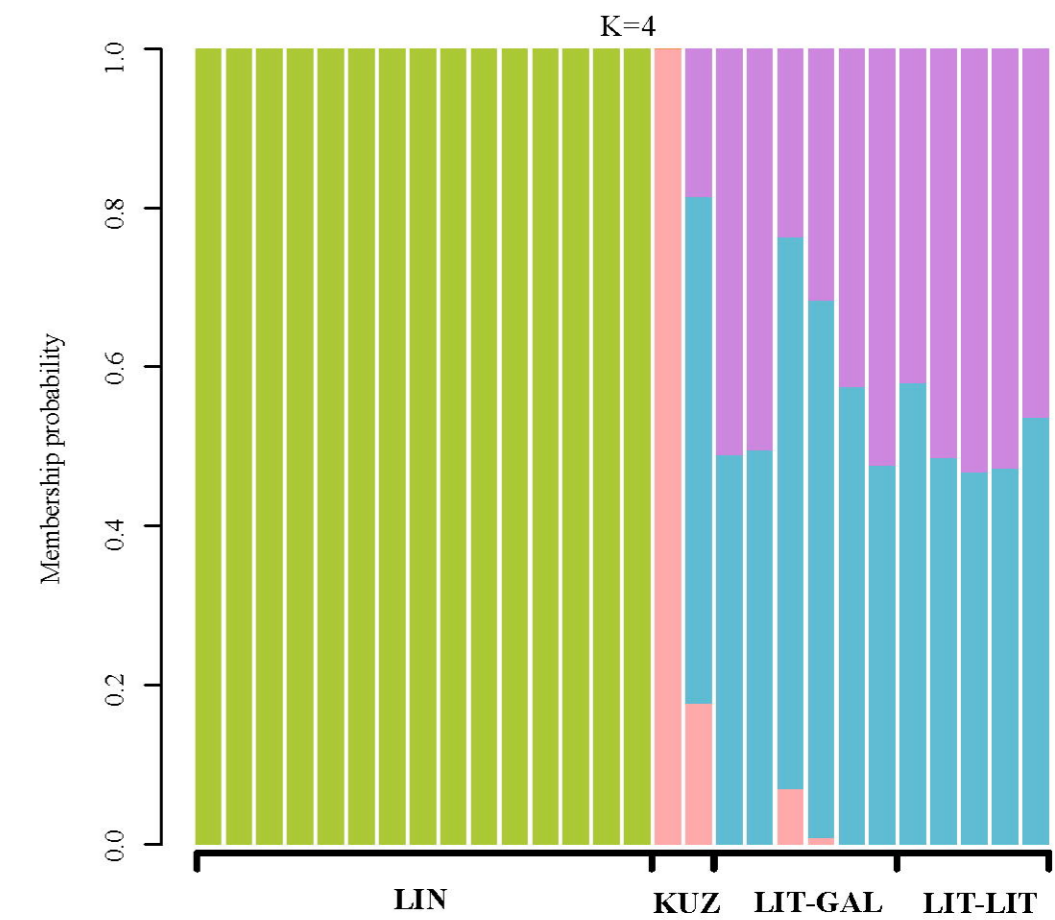
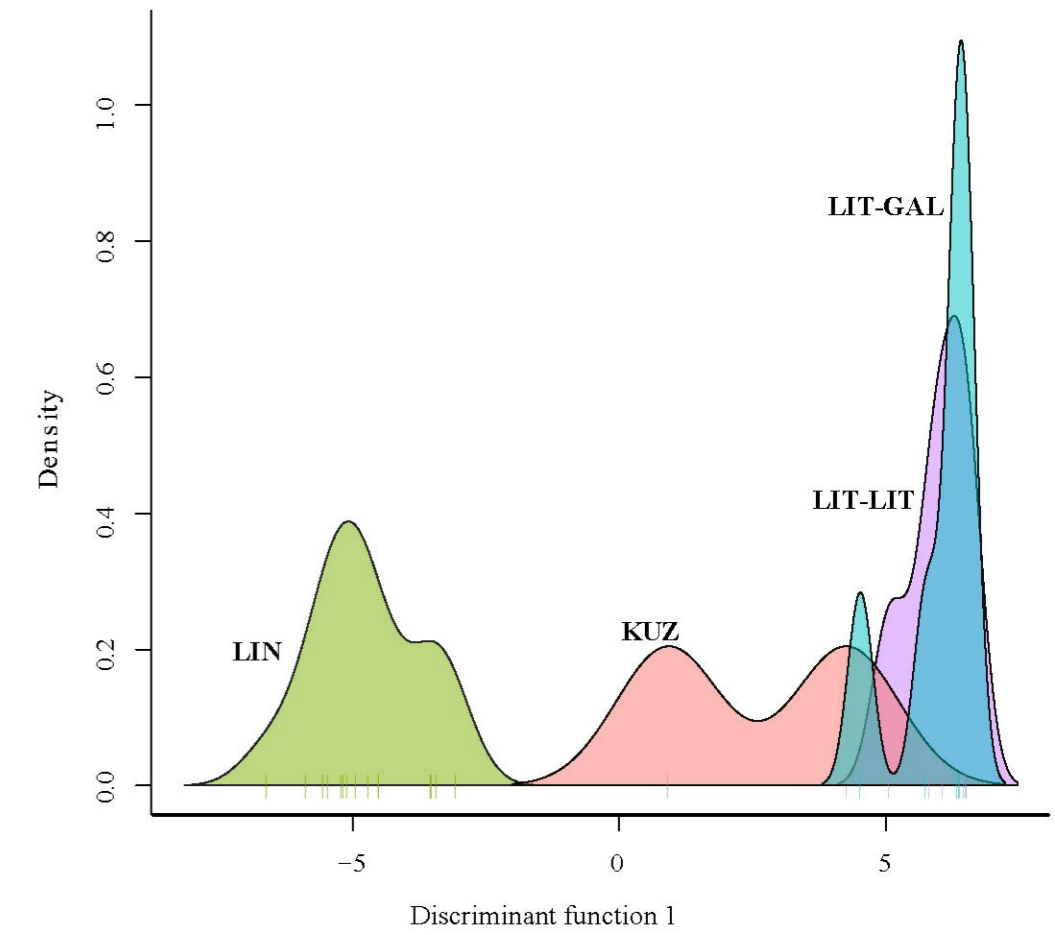
bioRxiv preprint doi: <https://doi.org/10.1101/823641>; this version posted December 11, 2019. The copyright holder for this preprint (which was not certified by peer review) is the author/funder, who has granted bioRxiv a license to display the preprint in perpetuity. It is made available under aCC-BY-NC-ND 4.0 International license.



(b) Niche overlap



(c) Genetic clustering



Last interglacial
(120,000 - 140,000
yr BP)

**Last Glacial
Maximum**
(21,000 yr BP)

Present

LIN



KUZ



LIT-GAL



LIT-LIT

